PHYSICAL REVIEW B VOLUME 5, NUMBER 7 1 APRIL 1972

Microscopic Description of Electron-Solid Interactions at a Surface*

Peter J. Feibelman
Department of Physics, University of Illinois, Urbana, Illinois 61801
and State University of New York, Stony Brook, New York 11790

and

C. B. Duke and A. Bagchi†
Department of Physics, Materials Research Laboratory and Coordinated Science Laboratory, University of Illinois, Urbana, Illinois 61801

(Received 15 November 1971)

A microscopic quantum theory of the scattering of an electron at metal-vacuum interfaces is constructed. The interactions of the electron with the short-range electron-ion core potential, the bulk-density fluctuations (e.g., plasmons), and the induced surface charge all are incorporated into the theory in a systematic fashion. Models of the surface- and bulk-charge-density fluctuations are catalogued as appropriate limiting cases of theory. The structure and predictions of the various models are compared, and the suitability of the models as the basis of a theory of electron-solid scattering is examined. The approximations required to produce from the general theory the usual semiclassical description of bulk- and surface-plasmon emission by keV electron transmission are displayed. Similarly, the theory is applied to "derive" the model Hamiltonian recently used to construct a semiphenomenological quantum-field theory of inelastic low-energy ($10 \lesssim E \lesssim 10^3$ eV) electron diffraction. A distorted-wave-scattering theory of elastic low-energy electron diffraction is proposed in which bulk- and surface-plasmon inelastic processes appear as loss terms in a nonlocal complex optical potential whose nature is examined in detail. In appropriate limits, the optical potential is shown to lead both to the image force and to the empirical local-potential models which have been used in calculating elastic low-energy electron diffraction. The pronounced differences between the empirical models and the predictions of the microscopic theory for the optical potential are explored. Some of the consequences of these differences for the analysis of experimental elastic–low-energy–electron-diffraction data are derived.

I. INTRODUCTION

Recent studies of both elastic[1–7] and inelastic[8,9] low-energy electron diffraction (ELEED and ILEED, respectively) have improved the theoretical description of these phenomena to the extent that their applications to characterize the surface of a solid are becoming quantitative in nature. The ELEED data can be analyzed to determine the geometry of the surface atoms[1,10–12] and the ILEED data to determine the dispersion relation and damping of the loss modes excited by the scattered electron.[9,13,14] All of the models used in these analyses embody essentially phenomenological descriptions of the interaction of the electron with the excitations of the solid. In particular, the effect of surface-plasmon loss processes on ELEED cross sections, although long suspected to be important,[1,2,15] is known[8] not to be described adequately (if at all) by existing models. This fact leads to difficulties in using these models to characterize quantitatively the properties of a surface. For example, the absolute intensities of different ELEED beams predicted by otherwise adequate model calculations are in disagreement with existing data,[6,7] and the dependence on the angle of incidence and crystal face of these intensities is not described quantitatively by current model calculations.[7,16,17] Similar problems in describing the details of the data occur in analyses of ILEED intensities,[13,14,17] although the model calculations of these processes are not yet as refined as those of ELEED. The theory reported in this paper is presented as a first step in resolving such difficulties by virtue of constructing as an appropriate basis for the theoretical data analysis a model in which both surface and bulk loss processes are incorporated *a priori* on an equal footing. Although we have not yet carried our calculations as far as those of the phenomenological models, we are able to demonstrate that a microscopic treatment of surface excitations provides mechanisms of the proper nature and magnitude to remove some of the discrepancies noted above.

Our description of electron-solid interactions is based on the random-phase approximation (RPA) to the linear response of the solid to the electromagnetic field of the electron. Relativistic retardation phenomena are neglected *a priori*. The literature on the linear response of a semi-infinite medium to an external electric field is substantial.[18–24] We adopt the formalism of Feibelman[19] because his use of the spectral decomposition of the linear-response operator is ideally suited for our calculations of the electron-density-fluctuation vertex function for

all of the independent density fluctuations of the system. This formalism is specified, using a generalized state-vector notation appropriate for our applications, in Sec. II.

Inspection of the considerable literature on surface-plasmon phenomena[25] quickly reveals the use of a variety of models whose relationships with each other are not apparent. Therefore, as one of our main tasks is the evaluation within our quantum theory of the electron-plasmon-interaction vertex, in Sec. III we classify these models, establish their interrelations, and evaluate the density-fluctuation excitation spectra and state vectors for two of them. In particular, we develop the results for the "step-density" model in detail (Sec. III B) because it provides the connecting link between the microscopic quantum theory and the semiclassical phenomenological models of electron-plasmon interactions. This link subsequently is established in Sec. IV A. Since one of the unique features of the formalism, the orthogonality and completeness of the density-fluctuation modes, is to play a crucial role in our evaluation of the electron-solid optical potential, we verify in Sec. IV A that it leads to a directly observable phenomenon: the reduction of the forward-scattering cross section for the bulk-plasmon-assisted transmission of keV electrons through thin films. The step-density model's prediction of this effect is calculated and shown to agree with both experimental data[26] and the hydrodynamical-model calculation of Ritchie.[27] Therefore we consider this important aspect of our microscopic analysis to be firmly established.

In Sec. V we turn to our major task: the application of the microscopic quantum analysis to describe ELEED. The outline of an appropriate distorted-wave multiple-scattering theory is given in Sec. V A, together with our expression for the electron-solid optical potential. As in the case of surface plasmons, a sizable literature exists on alternative schemes (mostly semiclassical) for evaluating such a potential. Therefore in Sec. V B we classify these procedures and relate them to the expression predicted by our quantum theory. In Sec. V C we show how to recover from our formalism the conventional empirical descriptions[1-7] of the absorptive part of the optical potential. A few previously unnoticed consequences of such descriptions are discussed in this subsection. In Sec. V D we calculate the optical potential using the step-density model and demonstrate that in the semiclassical limit the model gives the image force outside the metal and a short-range force inside the metal. Finally, in Sec. V E we develop an approximate solution of the Schrödinger equation which describes electronic motion under the influence of the optical potential associated with the step-density model and demonstrate that, even in the quantum theory, far outside the metal an electron acts "as if" it were under the influence of the classical image force. However, due to the long-range nonlocality of the optical potential predicted by the microscopic theory, conventional methods do not enable us to solve the associated Schrödinger equation in all of coordinate space; i.e., our approximate solution is only valid sufficiently far from the surface. Consequently the evaluation of elastic electron-solid cross sections, even for a highly simplified model of the solid, remains an interesting and open problem.

Because of the extensive nature both of our internal checks of the quantum theory and the establishment of its relation to substantial bodies of the literature, we have endeavored to make each section as self-contained as possible. By inspection of the above outline the interested reader can isolate and examine those sections of interest to him without reading the whole paper. A synopsis of our new results is given in Sec. VI.

II. REVIEW OF FORMALISM

Let us assume that an electron impinges on a solid with sufficiently high energy that the Born approximation is valid in describing its coupling to the excitations of the solid. The inelastic electron-scattering cross section is then simply an integral over the linear-response functions of the solid.[28]

The earliest descriptions of the linear response of a solid with a surface[27,29] were based on a semiclassical approach, which was basically hydrodynamic. More recently, several authors[18-24] have employed the RPA, a fully quantum-mechanical approach to linear-response theory. In this section we discuss the linear response of a solid with a surface from a point of view that is sufficiently general to permit the codification of all previous work on the problem.[30] As illustrations, in Sec. II we will discuss two model surfaces, the step-function-density model,[19] and the infinite-square-barrier model for which Beck and Heger and Wagner have recently obtained numerically the surface component of the exact RPA linear-response function.[31]

We restrict our description of the solid, for ease of presentation, to the jellium model, in which the (static) positive-charge background is isotropic in the interior and falls to zero in some way at the surface. We further assume our solid to have the symmetry of a slab; the normal to the surface is taken to be in the z direction. Under these conditions, the response of the solid to a weak external potential $V_{\mathrm{EXT}}(\vec{q}, z, \omega)$ of wave vector $\vec{q}$ in the x-y plane, and a frequency ω, is given in the RPA as the induced electron-number density,

$$n^{(1)}(\vec{q}, z, \omega) = \int dz' \, \mathcal{L}(\vec{q}; z, z'; \omega)$$

$$\times[\int dz'' f_q(z'-z'')\, n^{(1)}(\vec{q}, z'', \omega) + V_{\mathrm{EXT}}(\vec{q}, z', \omega)] , \tag{1}$$

where the two-dimensional Fourier transform of the Coulomb interaction is denoted by

$$f_q(z'-z'') \equiv (2\pi e^2/q)\, e^{-q|z'-z''|} , \tag{2}$$

and the particle-hole propagator is

$$\mathfrak{L}(\vec{q};\ z,\ z';\ \omega) = 2\int \frac{d^2k}{(2\pi)^2} \sum_{nn'} \frac{\theta_{kn'} - \theta_{k+qn}}{\omega - \omega_{k+qn} + \omega_{kn'}} \times \psi_n(z)\psi_{n'}^*(z)\psi_{n'}(z')\psi_n^*(z') . \tag{3}$$

In Eq. (3) we have defined $\theta_{kn} = \theta(\epsilon_F - \omega_{kn})$, where ϵ_F is the electron Fermi energy and $\theta(x)$ is the unit step function. The energy ω_{kn} is defined by

$$\omega_n = k^2/2m + \omega_n , \tag{4}$$

$k^2/2m$ being the energy of plane-wave state $e^{i\vec{k}\cdot\vec{x}}$ of motion parallel to the slab surface and ω_n being the energy associated with the single-particle wave function $\psi_n(z)$, according to the Schrödinger equation

$$-\frac{1}{2m}\frac{d^2\psi_n}{dz^2} + V(z)\psi_n(z) = \omega_n\psi_n(z) . \tag{5}$$

In principle, the potential $V(z)$ is to be derived self-consistently by solving the Hartree equation

$$V(z) = V_H(z) = -2\pi e^2 \int dz'\, |z-z'|\,[n_0(z') - n_B(z')] , \tag{6}$$

where $n_B(z)$ is the assumed background positive-density profile and $n_0(z)$ is the self-consistent electron-number density[32]

$$n_0(z) = 2\int \frac{d^2k}{(2\pi)^2} \sum_n \theta_{kn} |\psi_n(z)|^2 . \tag{7}$$

In practice, however, the Hartree equations are not solved[33]; $V(z)$ is chosen arbitrarily, and is used to determine a set of single-particle wave functions according to Eq. (5). In the work of Fedders,[18] and, more recently, of Beck[22,31a,34] and collaborators, $V(z)$ is taken to be an infinite square barrier. Although this choice is unrealistic, it has the advantage of rendering Eq. (1) soluble with a minimum of labor. In the work of Feibelman,[19,35,36] an attempt is made to search for properties of the solution to Eq. (1) which depend only on the gross features of the ground-state many-electron wave function, such as the density profile given by Eq. (7). Quantities such as the dispersion and attenuation of the surface plasmon require a more detailed knowledge of the ground-state wave function, however. Therefore it is necessary to study realistic models of $V(z)$ to obtain reliable results.[36]

In order to express the solution to Eq. (1) in a general form, we rewrite the equation in operator notation,

$$|n_{q\omega}^{(1)}\rangle = \mathfrak{L}_{q\omega}[\, f_q |n_{q\omega}^{(1)}\rangle + |V_{\mathrm{EXT}}(q\omega)\rangle] , \tag{8}$$

where $\mathfrak{L}_{q\omega}$ is the operator whose coordinate-space representation $\langle z|\mathfrak{L}_{q\omega}|z'\rangle$ is the particle-hole kernel of Eq. (3), $\mathfrak{L}(\vec{q};\ z,\ z';\ \omega)$, and similarly f_q is the operator corresponding to the Coulomb interaction, cf. Eq. (2). For ω on the imaginary axis, $\mathfrak{L}_{q\omega}$ is a Hermitian operator,[37] and therefore Eq. (8) may be solved for imaginary ω by expansion in the appropriate complete basis, the set of functions satisfying

$$\mathfrak{L}_{q\omega} f_q |u_l(q\omega)\rangle = \lambda_l(q\omega)|u_l(q\omega)\rangle . \tag{9}$$

To make correspondence with the ordinary theory of integral equations with Hermitian kernels, we must symmetrize Eq. (9). This is particularly simple, since f_q is a positive definite operator. We define[38] the operator $f_q^{1/2}$ by

$$f_q^{1/2} f_q^{1/2} = f_q . \tag{10}$$

Let

$$\begin{aligned} |v_l(q\omega)\rangle &\equiv f_q^{1/2}|u_l(q\omega)\rangle , \\ \mathfrak{K}_{q\omega} &= f_q^{1/2}\,\mathfrak{L}_{q\omega} f_q^{1/2} . \end{aligned} \tag{11}$$

Then Eq. (9) becomes

$$\mathfrak{K}_{q\omega}|v_l(q\omega)\rangle = \lambda_l(q\omega)|v_l(q\omega)\rangle , \tag{12}$$

where $\mathfrak{K}_{q\omega}$ is a Hermitian kernel for imaginary ω. (Results for real ω are obtained by analytic extention.) It follows that the $|v_l\rangle$ form a complete orthogonal set, i.e., that the identity operator I may be written as

$$I = \sum_l \frac{|v_l(q\omega)\rangle\langle v_l(q\omega)|}{\langle v_l(q\omega)|v_l(q\omega)\rangle} , \tag{13}$$

and that the $|v_l(q\omega)\rangle$ corresponding to different $\lambda_l(q\omega)$ satisfy

$$\langle v_l(q\omega)|v_{l'}(q\omega)\rangle = \int dz\, v_l^*(qz\omega)v_{l'}(qz\omega) = \delta_{ll'}\mathfrak{N}_l(q\omega), \tag{14}$$

where $\mathfrak{N}_l$ is a normalization constant. It also follows that the operator $\mathfrak{K}_{q\omega}$ has the expansion

$$\mathfrak{K}_{q\omega} = \sum_l \lambda_l(q\omega) \frac{|v_l(q\omega)\rangle\langle v_l(q\omega)|}{\mathfrak{N}_l(q\omega)} . \tag{15}$$

At this point we have the tools necessary to solve Eq. (8) formally. We expand

$$\begin{aligned} f_q^{1/2}|n_{q\omega}^{(1)}\rangle &= \sum_l c_l(q\omega)|v_l(q\omega)\rangle , \\ f_q^{-1/2}|V_{\mathrm{EXT}}(q\omega)\rangle &= \sum_l V_l(q\omega)|v_l(q\omega)\rangle . \end{aligned} \tag{16}$$

Substituting Eqs. (16) in Eq. (8), multiplying both sides of the resulting equation by $f_q^{1/2}$, and using Eq. (12), we obtain

$$\sum_l \lambda_l(q\omega)[c_l(q\omega) + V_l(q\omega)]\,|v_l(q\omega)\rangle = \sum_l c_l|v_l(q\omega)\rangle . \tag{17}$$

Making use of the orthogonality, Eq. (14), of the

$|v_l\rangle$, we thus find

$$c_l(q,\omega)=\lambda_l(q\omega)V_l(q\omega)/[1-\lambda_l(q\omega)]\ . \tag{18}$$

The second of Eqs. (16) implies that

$$V_l(q\omega)=\langle v_l(q\omega)|\,f_q^{-1/2}|\,V_{\rm EXT}(q\omega)\rangle\ . \tag{19}$$

Substituting Eq. (19) in Eq. (18), and substituting the result in the first of Eqs. (16), we obtain the formal solution to the RPA equation, Eq. (8),

$$|n_{q\omega}^{(1)}\rangle=\sum_l \frac{1}{\mathfrak{N}_l(q\omega)}\frac{\lambda_l(q\omega)}{1-\lambda_l(q\omega)} \times f_q^{-1/2}|v_l(q\omega)\rangle\langle v_l(q\omega)|\,f_q^{-1/2}|\,V_{\rm EXT}(q\omega)\rangle\ . \tag{20}$$

Returning to the u via the definition, Eq. (11), this result may be rewritten

$$|n_{q\omega}^{(1)}\rangle=\sum_l \frac{1}{\mathfrak{N}_l(q\omega)}\frac{\lambda_l(q\omega)}{1-\lambda_l(q\omega)} \times|u_l(q\omega)\rangle\langle u_l(q\omega)|\,V_{\rm EXT}(q\omega)\rangle\ . \tag{21}$$

Equation (21) looks simpler than Eq. (20) because it is written in terms of the $|u_l\rangle$, which have a simply physical interpretation as the normal-mode electron-density-fluctuation-state functions. In terms of the $|u_l\rangle$, the mathematics is somewhat messier, but in general, the physical interpretation is more straightforward.

Let us now explore the meaning of Eq. (21). Functional differentiation of Eq. (21) yields

$$\frac{\delta n_{q\omega}^{(1)}}{\delta V_{\rm EXT}(q\omega)}\equiv \mathcal{S}_{q\omega}=\sum_l \frac{1}{\mathfrak{N}_l(q\omega)}\frac{\lambda_l(q\omega)}{1-\lambda_l(q\omega)} \times|u_l(q\omega)\rangle\langle u_l(q\omega)|\,, \tag{22}$$

where $\mathcal{S}_{q\omega}$ is the "density-density response function" of the solid. The poles of $\mathcal{S}_{q\omega}$ correspond to the resonances of the solid, the modes of oscillation which can be excited by a weak external probe. Referring to Eq. (22), we see that the lth mode occurs at a frequency given by

$$\lambda_l(q\omega)=1\ , \tag{23}$$

and corresponds to the excitation of an electron-number-density fluctuation (in coordinate space)

$$u_l(qz\omega)=\langle z|\,u_l(q\omega)\rangle\ . \tag{24}$$

In principle, the u_l may be calculated by solving the eigenvalue equation (9). To date, however, this equation has only been solved for certain highly simplified models of the electron distribution at the jellium surface, for which $\mathcal{L}_{q\omega}$ in a fairly simple operator. (These models are discussed in Sec. III.) Nevertheless, we can guess what the approximate forms of the various u_l's and values of the λ_l's must be. For example, the surface plasmon corresponds to a $u(z)$ which behaves like a δ function near the solid surface (since it is a "surface-charge" fluctuation, see Fig. 1), and a $\lambda_l\approx\omega_p^2/2\omega^2$ for long wavelengths, where ω_p is the classical plasma frequency. Similarly, we would expect the $u_l(z)$ corresponding to bulk plasmons to be sinusoidally varying functions in the solid, with the index l corresponding to the wave number of the sinusoidal variation. The corresponding λ_l should be equal to ω_p^2/ω^2 plus dispersive corrections.

Given a $u(z)$ guessed from physical considerations, we may evaluate the corresponding $\lambda(q\omega)$. Using Eqs. (11), (12), (14), and (3), we obtain

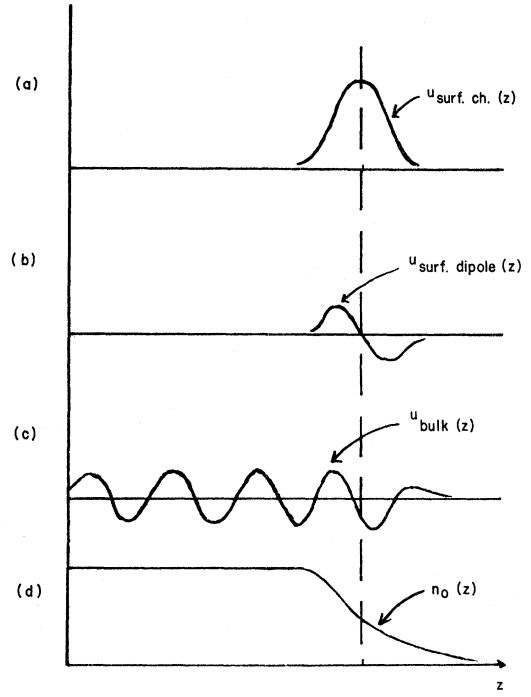

FIG. 1. Schematic drawings of charge-density-fluctuation profiles for the various modes of excitation. Curve (a) represents a surface-charge or "surface-monopole" fluctuation. Curve (b) represents a surface-dipole oscillation and curve (c) a bulk-charge mode. The ground-state electron density $n_0(z)$ is shown in curve (d).

$$\lambda_l(q\omega)=2\int\frac{d^2k}{(2\pi)^2}\sum_{nn'}\frac{\theta_{kn'}-\theta_{k+qn}}{\omega-\omega_{k+qn}+\omega_{kn'}}\left|\int dz\,dz'\,\psi_n^*(z)\psi_{n'}(z)f_q(z-z')u_l(qz'\omega)\right|^2\Big/\int dz\,dz'\,u_l^*(qz\omega)f_q(z-z')u_l(qz'\omega)\ . \tag{25}$$

Equation (25) may be utilized as the basis of a variational calculation of the u_l and λ_l. The functional equation

$$\delta\lambda_l(q\omega)/\delta u_l(qz\omega) = 0 \tag{26}$$

is equivalent to Eq. (9). Since it is easy to guess plausible forms of the u, the variational approach may prove to be a useful calculational tool, despite the fact that it requires the solution of the nontrivial problem of analytic extension of the u_l's and λ_l's from the imaginary to the real ω axis. In fact, a surface-plasmon calculation which is based on Eq. (26) is now in progress.[39]

The physical meaning of the dispersion relation $\lambda(q\omega) = 1$, Eq. (23), is revealed by examining the high-frequency limit. Using Eq. (25), we find that

$$\lambda_l(q,\ \omega\to\infty) \to \frac{1}{2m\omega^2}\int dz\, n_0(z)\left(q^2\left|\phi_l(qz\omega)\right|^2 + \left|\frac{d\phi_l(qz\omega)}{dz}\right|^2\right) \Big/ \tfrac{1}{2}\int dz\, u_l^*(qz\omega)\phi_l(qz\omega)\,, \tag{27}$$

where

$$\phi_l(qz\omega) \equiv \int dz'\, f_q(z-z')u_l(qz'\omega) \tag{28}$$

is the electron charge e times the potential associated with the electron-density fluctuation u_l. In deriving Eq. (27) we have used the completeness of the ψ_n and the definition of $n_0(z)$ [Eq. (7)].

We now show that the numerator and denominator in Eq. (27) are, respectively, the kinetic and potential energies associated with the motion of the electron that produces the density fluctuation u_l. Thus the dispersion relation $\lambda_l(q\omega) = 1$ is the condition for harmonic oscillation, namely, that the potential energy associated with the electron-density fluctuation equal the kinetic energy. The demonstration is based on a linearized hydrodynamic picture. If, for a particular mode l, the local electron velocity and number density are given, respectively, by $\vec{w}_l(qz\omega)$ and $n_l(q,\ z,\ \omega) = n_0(z) + u_l(qz\omega)$, then the kinetic energy of the mode, to lowest order in fluctuating quantities, is

$$T_l(q\omega) = \tfrac{1}{2}m\int dz\, n_0(z)\left|\vec{w}_l(qz\omega)\right|^2 . \tag{29}$$

However, according to Euler's equation (Newton's second law applied to hydrodynamics), again to lowest order,

$$m\frac{\partial\vec{w}_l(\vec{x},\ z,\ t)}{\partial t} = -\nabla\phi_l(\vec{x},\ z,\ t)\,, \tag{30}$$

where $\phi_l(x,\ z,\ t)$ is the potential that drives the electron motion.[40] Fourier transforming Eq. (30) in $\vec{x}$ and t, and squaring, we obtain

$$\left|\vec{w}_l(qz\omega)\right|^2 = \frac{1}{m^2\omega^2}\left(q^2\left|\phi_l(qz\omega)\right|^2 + \left|\frac{d\phi_l(qz\omega)}{dz}\right|^2\right) . \tag{31}$$

Substituting Eq. (31) in Eq. (29), we verify that the numerator of Eq. (27) is the kinetic energy corresponding to the mode l. That the denominator of Eq. (27) is the corresponding potential energy is obvious by inspection, using the definitions Eqs. (28) and (2).

Finally, let us take note of a useful consequence of the orthogonality relation Eq. (14). Essentially, this relation tells us that the various $u_l(z)$'s are distinguished by their respective number of zeros; that is, different u_l's must have different numbers of zeros in order to satisfy Eq. (14). This result is useful because it enables us to classify the u_l's according to the respective ranges outside the solid surface at which their fields may be felt.

There are two classes of u_l for a semi-infinite slab, those having a finite number of zeros and those having an infinite number of them. The latter class of $u_l(z)$ comprises a continuum, for which the index l may be replaced by the wave number κ; this class $[u_\kappa^{(B)}(z)]$ corresponds to the bulk excitations of the solid. The former class presumably comprises only a small number of $u_l^{(S)}(z)$, for which the index l may simply be taken to equal the number of nodes. These $u_l^{(S)}$ are localized near the surface and correspond to the surface excitations of the solid.

Using Eq. (28) we may evaluate the potential corresponding to a given $u_l(z)$. It is easy to see that the potential due to $u_0^{(S)}(z)$, the surface-charge mode, has a longer-range potential than that associated with the surface-dipole mode $u_1^{(S)}(z)$, and so forth. The potential due to the bulk modes is essentially zero outside the solid, since the bulk $u_\kappa^{(B)}(z)$ are orthogonal to all the surface modes, those which give rise to the longest-range potentials. These remarks will be illustrated in the context of specific models in Sec. III.

The fact that $u_0^{(S)}(z)$ alone gives rise to the longest-range coupling between a charged particle and a solid surface is important, because it provides a basis for the microscopic theory of the corrections to the image force, which is the only force acting on such a particle at sufficiently large distances from the surface. This has been discussed previously in a formal way,[41] and is dealt with below in the context of a simple model (Sec. V).

III. APPLICATION TO MODELS

A. Model Classification

Our aim in this section is to discuss the two

models for which the microscopic theory, developed above, has been worked out in detail. In order to permit an assessment of the relative significance of these calculations, however, we begin by classifying models according to the nature and degree of approximation that they involve.

a. Full RPA models. A full RPA model of collective excitations at a surface involves the solution of the eigenvalue equation (9). Different such models correspond to different choices of the potential $V(z)$. The word "full" is meant to distinguish models based on solving Eq. (9) directly from those (see Sec. III A *b*) in which the kernel $\mathfrak{L}_{q\omega}$ of Eq. (9) is expanded in q and/or ω^{-1} *before* the solution of Eq. (9) is carried out. To date the only full RPA model that has been solved[31] is that of the infinite wall

$$V(z)=\begin{cases}0\ , & z>0\\ \infty\ , & z<0\ .\end{cases}$$

Although this model is microscopic, it is not very realistic. The comparison of its predictions with experiment[14] shows that, indeed, it must be improved upon.

b. High-frequency microscopic models. In view of the fact that the surface- and bulk-plasmon energies are fairly high (~ 10 eV) compared to those of typical particle-hole states (~ 1 eV), one attempts, *before solving Eq.* (9), to expand $\mathfrak{L}_{q\omega}$ about its large-ω limit, retaining only the lowest-order terms. In this way one obtains an approximate $\mathfrak{L}_{q\omega}$, appropriate for determining the large-ω solutions to Eq. (1), which has two desirable features: (i) It is a differential rather than an integral operator; (ii) it is specified by a few average ground-state properties such as the electron-density profile and stress tensor. It is found, however, that the high-frequency approximation is internally consistent (for a metal-vacuum interface) only if the electron-density profile is taken to be a step function at the jellium surface. Thus there is only one possible high-frequency model of a metal-vacuum interface, and not a very realistic one at that.

High-frequency models, by their very nature, do not describe the small-ω solutions to Eq. (1). Thus they are useless in the study of the interaction of slow ($v<v_F$) external probes with solid surfaces. Full RPA calculations, on the other hand, are in principle valid in any frequency range.

c. Hydrodynamic models. The simplest, and historically the first, way of obtaining equations of motion for a bounded electron gas is to combine hydrodynamics with Maxwell's equations. If the electron gas is assumed to have a step-function density profile, and if plasmon dispersion is neglected, then the resulting equations are identical to those of the RPA high-frequency model [keeping terms up to $O(1/\omega^2)$ in the latter].

In order to evaluate dispersive effects, however, it is necessary to close the hydrodynamic equations by the introduction of a "constitutive relation," which relates pressure to the density fluctuations in the electron gas. (Neglecting dispersion corresponds to neglecting the term in Euler's equation corresponding to the *internal* pressure gradient.) Generally, the constitutive relation is chosen so that the hydrodynamic and RPA values of the bulk-plasmon dispersion agree. This choice does not, however, guarantee that the two models also agree on the value of the surface-plasmon dispersion.[42]

Recently the hydrodynamic equations have been applied to a model surface more realistic than the step-function density profile, namely, a density profile with a linear dropoff.[43] The interesting result, in this case, is that under certain circumstances the surface plasmon can have negative dispersion at long wavelengths. Nevertheless, the assumption of a hydrodynamic boundary condition at the point where the electron density equals zero is thought to be unwarranted.[36] Thus, the hydrodynamic model like the high-frequency model probably should be applied only in the case of a step-function density.

The hydrodynamic model cannot be used to estimate surface collective-mode damping, although a viscosity parameter may be introduced to describe this effect *a posteriori*.

B. Solution of High-Frequency Step-Density Model

Ultimately, for any model surface, our aim is to determine the complete set of λ's and u's (i.e., the dispersion relations and coupling constants) for all values of q and ω. But if we are satisfied to limit our study to that of collective effects, it is appropriate to restrict our attention to the limits of long wavelengths ($q \ll k_F$, the Fermi wave number) and high frequencies ($\omega \gg$ "typical" particle-hole frequencies). The question then arises: Must we first solve Eq. (9) and only then allow ω to become large, or is it possible to let $\omega \to \infty$ first and then solve for the dispersion relations of the collective modes? The idea of first expanding $\mathfrak{L}(\vec{q};\ z,\ z';\ \omega)$ in powers of $1/\omega$ is an attractive one, since [see Eq. (3)] once the expansion is made formally, the completeness of the ψ_n may be used to reduce the expression for $\mathfrak{L}$ to one involving only average properties of the unperturbed surface, such as the electron-density profile[19] $n_0(z)$. However, Feibelman recently has shown[26] that the neglect of particle-hole energies compared to typical collective-mode energies $\hbar\omega$, the assumption which is necessary if we are to expand $\mathfrak{L}$, is consistent only if $n_0(z)$ is chosen to be a step-function, i.e., $n_0(z)=n_\infty\theta(z)$. For any more realistic density profile, decay of the collective excitation into particle-hole states must be taken into account from the beginning.

Thus, as our first example, let us obtain the complete set of u_l's and λ_l's for the step-function density in the high-frequency limit. For the details of the derivation, we refer to the original article on the high-frequency approximation.[19] Equation (9) is multiplied on both sides by f_q, yielding an equivalent equation for ϕ_l,

$$f_l \mathcal{L}_{q\omega} | \phi_l(q\omega)\rangle = \lambda_l(q\omega) | \phi_l(q\omega)\rangle \ . \tag{32}$$

$\mathcal{L}_{q\omega}$ is expanded in powers of $1/\omega$. One keeps only the lowest nonvanishing term in the expansion. Using the completeness of the ψ_n, one then obtains [cf. Eq. (21) of Ref. 19]

$$\lambda_l(q\omega)\phi_l(qz\omega) = \frac{2\pi e^2}{m\omega^2}\int dz' \, e^{-q|z-z'|} n_0(z') \times \left(q\phi_l(qz'\omega) + \mathrm{sgn}(z-z') \frac{d\phi_l(qz'\omega)}{dz'} \right). \tag{33}$$

It is worth noting[44] that Eq. (33), with $\lambda_l(q\omega)$ taken equal to 1, is just the equation of motion we obtain if we consider the electron field hydrodynamically. We simply combine the equation of continuity

$$\vec{\nabla} \cdot [n_0(z)\vec{w}(\vec{x}, z, t)] = -\frac{\partial u(x, z, t)}{\partial t} \tag{34}$$

with the (hydrodynamic) Euler equation (30), yielding

$$\frac{\partial^2 u(\vec{x}, z, t)}{\partial t^2} = \frac{1}{m} \vec{\nabla} \cdot [n_0(z) \vec{\nabla} \phi(\vec{x}, z, t)] \ . \tag{35}$$

Fourier transforming in $\vec{x}$ and t, and using the relation Eq. (28), we obtain

$$\phi(qz\omega) = \frac{2\pi e^2}{qm\omega^2}\int dz' \, e^{-q|z-z'|} \times \left[q^2 n_0(z')\phi(z') - \frac{d}{dz'}\left(n_0(z') \frac{d\phi(qz'\omega)}{dz'} \right) \right], \tag{36}$$

which is identical to Eq. (33), after an integration by parts and with $\lambda = 1$. This proves that the hydrodynamic description of the collective modes is identical to that of the RPA expanded through terms of $O(1/\omega^2)$. The physical interpretation of this identity is that when the frequency of a collective mode is high compared to typical frequencies of particle and hole motion, electrons must respond to the local instantaneous (self-consistent) electric field. But response to the instantaneous (rather than time-delayed) electric field is precisely the content of the Euler equation.

The reasons for the breakdown of the high-frequency approximation when $n_0(z)$ is chosen to be a realistic (i.e., continuous) function of z have been treated elsewhere. Here, we set

$$n_0(z) \equiv n_\infty \theta(z) \tag{37}$$

and proceed to solve Eq. (33). Substituting Eq. (37) in Eq. (33) and integrating by parts, we obtain

$$\frac{m\omega^2}{2\pi e^2 n_\infty} \lambda_l(q\omega)\phi_l(qz\omega) = \begin{cases} 2\phi_l(qz\omega) - \phi_l(q0\omega)\, e^{-qz} & z > 0 \\ \phi_l(q0\omega) e^{qz} & z < 0 \end{cases} . \tag{38}$$

Equation (38) admits two types of solution. If $\phi_l(q0\omega) \neq 0$, then

$$\phi_l(qz\omega) = \phi_l(q0\omega)\, e^{-q|z|} \ , \qquad \lambda_l(q\omega) = \frac{\omega_p^2}{2\omega^2} \ , \tag{39}$$

where $\omega_p^2 = 4\pi e^2 n_\infty / m$ is just the classical plasma frequency. This solution corresponds to the surface plasmon. The associated charge fluctuation is obtained from Eq. (28) to be

$$u_l^{(S)}(qz\omega) = \frac{1}{4\pi e^2}\left(q^2 - \frac{d^2}{dz^2} \right)\phi_l(qz\omega) = \frac{q\phi_l(q0\omega)}{2\pi e^2}\, \delta(z) \ , \tag{40}$$

which is localized precisely at the surface.[45] It is nodeless, and thus we assign it the index $l = 0$. The frequency of the surface plasmon is given by

$$1 = \lambda_0(q\omega) = \frac{\omega_p^2}{2\omega^2} \ , \tag{41}$$

which, not surprisingly, is the hydrodynamic result. There is no dispersion in Eq. (41), because we have retained only terms $O(1/\omega^2)$ in expanding the RPA kernel. For definiteness, we normalize $u_0^{(S)}$ by choosing $\phi_l(q0\omega) \equiv 2\pi e^2/q$. With this normalization, $u_0^{(S)}(qz\omega)$ has the dimensions of an electron-number-density fluctuation.

If $\phi_l(q0\omega) = 0$, we obtain from Eq. (38)

$$\phi_l(qz\omega) = \theta(z) \times \text{an arbitrary function of } z \text{ which approaches zero as } z \to 0^+, \qquad \lambda_l(q\omega) = \omega_p^2/\omega^2 \ . \tag{42}$$

These solutions correspond to the bulk plasmons.[45] The index l should be identified as the wave number κ. The frequency of the bulk plasmon is given by

$$1 = \lambda_\kappa(q\omega) = \omega_p^2/\omega^2 \ , \tag{43}$$

which is again independent of q and κ (i.e., dispersionless) because we have retained only terms $O(1/\omega^2)$. As a result of this degeneracy, i.e., the independence of $\lambda_\kappa(q, \omega)$ of q and κ, we are free to enumerate the $\phi_\kappa^{(B)}(qz\omega)$ in terms of any convenient complete set of states.

Using Eqs. (11) and (28), it is easy to see that the orthogonality condition Eq. (14) may be rewritten:

$$\int dz \, \phi_l(qz\omega) u_{l'}^*(qz\omega) = 0 \ , \quad l \neq l' \ . \tag{44}$$

Let l and l' refer to a bulk mode and the surface

mode, respectively. The orthogonality condition thus yields

$$\int dz\, \phi_\kappa^{(B)}(qz\omega)\, u_0^{(S)}(qz\omega) = 0 , \tag{44a}$$

which reduces, using Eq. (40), to the requirement that $\phi_\kappa^{(B)}(q, 0, \omega) = 0$. This requirement automatically is satisfied if we follow the prescription, Eq. (42), given above.

Our final problem is to ensure that the set of ϕ's chosen satisfies the completeness relation, Eq. (13). It is important to carry out this verification explicitly, in order to be certain that we have not left out any modes, e.g., a surface-dipole mode. Using Eqs. (11) and (28), together with Eq. (13), the completeness relation may be expressed in two equivalent forms:

$$\sum_l \frac{u_l(z) u_l^*(z')}{\mathfrak{N}_l} = f_q^{-1}(z - z') \equiv \frac{1}{4\pi e^2}\left(q^2 - \frac{d^2}{dz^2}\right)\delta(z - z'), \tag{45a}$$

$$\sum_l \frac{\phi_l(z)\, \phi_l^*(z')}{\mathfrak{N}_l} = f_q(z - z') = \frac{2\pi e^2}{q}\, e^{-q|z - z'|} . \tag{45b}$$

The equation

$$f_q^{-1}(z - z') \equiv \frac{1}{4\pi e^2}\left(q^2 - \frac{d^2}{dz^2}\right)\delta(z - z') \tag{46}$$

used in Eq. (45a) gives the explicit matrix inverse of the Coulomb interaction, which is defined by

$$\int dz'\, f_q^{-1}(z - z') f_q(z' - z'') \equiv \delta(z - z'') . \tag{47}$$

The fact that the right-hand side of Eq. (45a) is given simply in terms of a δ function suggests that we should try to fulfill the equation by expressing the $u_\kappa^{(B)}$ as sinusoidal functions. We therefore start from the *ansatz* for the bulk modes,

$$u_\kappa^{(B)}(qz\omega) = (\alpha_{\kappa q\omega} \sin \kappa z + \beta_{\kappa q\omega} \cos \kappa z)\theta(z) . \tag{48}$$

The coefficients $\alpha_{\kappa q\omega}$ and $\beta_{\kappa q\omega}$, however, are not independent. They must be related in such a way as to render

$$\phi_\kappa^{(B)}(q0\omega) = \frac{2\pi e^2}{q}\int_{-\infty}^{\infty} dz'\, e^{-q|z'|}\, u_\kappa^{(B)}(qz\omega) = 0 , \tag{49}$$

which ensures orthogonality to the surface mode. This condition is seen to be satisfied for the *ansatz* (48) if $\beta_{\kappa q\omega}/\alpha_{\kappa q\omega} = -\kappa/q$, or in other words, if

$$u_\kappa^{(B)}(qz\omega) \propto \theta(z)\left(q - \frac{d}{dz}\right) \sin \kappa z . \tag{50}$$

Incidentally, we may note that this choice of $u_\kappa^{(B)}$ automatically guarantees that the potential due to the bulk mode vanishes for $z < 0$, as is required [see Eq. (42)]. This follows according to

$$\phi_\kappa^{(B)}(qz < 0\omega) \propto \int_0^\infty dz'\, e^{-q|z - z'|}\, u_\kappa^{(B)}(qz'\omega) = e^{qz}\int_0^\infty dz'\, e^{-qz'}\, u_\kappa^{(B)}(qz'\omega) = 0 , \tag{51}$$

in which the last equality follows from Eq. (49). Thus the vanishing of the bulk-plasmon potential outside the solid may be ascribed to the orthogonality of the bulk and surface modes.

In order to see how to fulfill the completeness condition Eq. (45a), let us start from the completeness relation for the sine function,

$$\int_0^\infty \frac{2d\kappa}{\pi} \sin \kappa z \sin \kappa z' = \delta(z - z') - \delta(z + z') . \tag{52}$$

From Eq. (52) we deduce straightforwardly that

$$\int_0^\infty \frac{2d\kappa}{\pi}\left[\theta(z)\left(q - \frac{d}{dz}\right)\sin \kappa z\right]\left[\theta(z')\left(q - \frac{d}{dz'}\right)\sin \kappa z'\right] = \theta(z)\theta(z')\left[\left(q^2 - \frac{d^2}{dz^2}\right)\delta(z - z') - \left(q - \frac{d}{dz}\right)\left(q - \frac{d}{dz'}\right)\delta(z + z')\right] . \tag{53}$$

Comparing Eqs. (53) and (45a), the possibility of satisfying the latter with $u_\kappa^{(B)}$'s of the form given in Eq. (50) looks quite promising. There are, however, two difficulties which must be overcome. First, we must explain the presence of the factors $\theta(z)\theta(z')$ in Eq. (53); that is, we must explain how we expect to obtain a "complete set" of u, if we can only have charge fluctuations inside the metal ($z > 0$). Second, we must learn to deal with the multiple singularities that appear in the last term of the right-hand side of Eq. (53) in the neighborhood of $z = 0$, $z' = 0$.

The first difficulty is easy to overcome; it is a standard problem in the spectral theory of integral operators. Because the electrons in the ground state of our solid are confined to its interior, the kernel $\mathfrak{L}(q; z, z'; \omega)$ vanishes when z or z' is outside the solid. [In the unexpanded form of $\mathfrak{L}$, Eq. (3), this is seen to be true because at least one of the wave functions $\psi_n(z)$ and $\psi_{n'}(z)$ corresponds to a negative energy.] In the high-frequency-expanded RPA, cf. Eqs. (36) and (32), we have effectively

$$\mathfrak{L}(q; z, z'; \omega) = \frac{1}{m\omega^2}\left[q^2 n_0(z) - \frac{d}{dz}\left(n_0(z)\frac{d}{dz}\right)\right]\delta(z - z') ,$$

and $\mathfrak{L}$ vanishes for z or z' outside the solid since $n_0(z) \to 0$ there.

Therefore any function of z which vanishes inside the solid is a solution to Eq. (32), with $\lambda = 0$. The class of functions which we have left out of our enumeration of the solutions to Eq. (32) is therefore the class of zero-eigenvalue solutions. By virtue of Eq. (22), however, we see that these functions do not contribute to the density-density response function (the contribution of any mode u_l is propor-

tional to the corresponding λ_l). This is satisfying; we would not want unphysical charge fluctuation in the vacuum to contribute to any physically measurable quantity. The zero-eigenvalue modes there are important *only* in fulfilling the completeness relations.

The second difficulty, that of the singular behavior of Eq. (53) near $z=0$, $z'=0$, is best avoided by trying to fulfill the requirement of completeness in the form (45b) instead of (45a). Our working hypothesis is that the electron-density-fluctuation spectrum is represented by

$$u_0^{(S)}(qz\omega)=\delta(z)\ , \qquad \lambda_0^{(S)}=\frac{\omega_p^2}{2\omega^2}\ , \tag{54a}$$

$$u_\kappa^{(B)}(qz\omega)=\theta(z)\left(q-\frac{d}{dz}\right)\sin\kappa z\ , \qquad \lambda_0^{(B)}=\frac{\omega_p^2}{2\omega^2}\ , \tag{54b}$$

$$u_\kappa^{(U)}(qz\omega)=\theta(-z)\left(q+\frac{d}{dz}\right)\sin\kappa z\ , \qquad \lambda_0^{(U)}=0\ , \tag{54c}$$

where the $u_\kappa^{(U)}$ are the unphysical zero-eigenvalue modes. The corresponding potentials are easily calculated using Eqs. (28) and (2). We obtain

$$\phi_0^{(S)}(qz\omega)=\frac{2\pi e^2}{q}\,e^{-q|z|}\ , \tag{55a}$$

$$\phi_\kappa^{(B)}(qz\omega)=\frac{4\pi e^2}{\kappa^2+q^2}\left[\left(q-\frac{d}{dz}\right)\sin\kappa z+\kappa e^{-qz}\right]\theta(z)\ , \tag{55b}$$

$$\phi_\kappa^{(U)}(qz\omega)=\frac{4\pi e^2}{\kappa^2+q^2}\left[\left(q-\frac{d}{dz}\right)\sin\kappa z-\kappa e^{qz}\right]\theta(-z)\ . \tag{55c}$$

It is straightforward to check that these modes are mutually orthogonal in the sense of Eq. (44), which, we recall, requires

$$\int dz\,\phi_l(qz\omega)u_{l'}(qz\omega)=0$$

for $l\neq l'$. We have $\phi_\kappa^{(B)}(q0\omega)=\phi_\kappa^{(U)}(q0\omega)=0$ which, as we noted above, implies orthogonality of the bulk and unphysical modes to the surface mode. The fact that the $\phi^{(B)}=0$ for $z<0$, while the $u^{(U)}$ are only nonzero in this region, implies the orthogonality of bulk to the unphysical modes. The orthogonality of one bulk mode to another is also easy to verify:

$$\lim_{\delta\to0}\int_0^\infty dz\,e^{-\delta z}\left[\left(q-\frac{d}{dz}\right)\sin\kappa z+\kappa e^{-qz}\right]\left[\left(q-\frac{d}{dz}\right)\sin\kappa' z\right]$$
$$=\lim_{\delta\to0}\int_0^\infty dz\,e^{-\delta z}(q^2+\kappa^2)\sin\kappa z\sin\kappa' z=0\ ,\quad \kappa\neq\kappa'\ , \tag{56}$$

where the factor $e^{-\delta z}$ has been introduced to ensure convergence at ∞. The equality in Eq. (56) is derived using integration by parts. A similar equation holds for the unphysical modes.

We now establish the completeness of the ϕ's in the sense of Eq. (45b). It is a straightforward exercise in contour integration to verify, starting from Eqs. (55b) and (55c), that

$$\int_0^\infty\frac{d\kappa}{\pi}\,\phi_\kappa^{(B)}(qz\omega)\phi_\kappa^{(B)}(qz'\omega)=\frac{(2\pi e^2)^2}{q}$$
$$\times[e^{-q|z-z'|}-e^{-q(z+z')}]\theta(z)\theta(z')\ , \tag{57}$$

$$\int_0^\infty\frac{d\kappa}{\pi}\,\phi_\kappa^{(U)}(qz\omega)\,\phi_\kappa^{(U)}(qz'\omega)=\frac{(2\pi e^2)^2}{q}$$
$$\times[e^{-q|z-z'|}-e^{q(z+z')}]\,\theta(-z)\theta(-z')\ . \tag{58}$$

The normalization constant for the surface mode is given by

$$\mathfrak{N}_0^{(S)}(q\omega)=\int dz\,\phi_0^{(S)}(qz\omega)\,u_0^{(S)}(qz\omega)=\frac{2\pi e^2}{q}\ . \tag{59}$$

Therefore the contribution of the surface mode to the sum of Eq. (45b) is

$$\frac{\phi_0^{(S)}(qz\omega)\phi_0^{(S)}(qz'\omega)}{\mathfrak{N}_0^{(S)}(q\omega)}=\frac{2\pi e^2}{q}\,e^{-q(|z|+|z'|)}\ . \tag{60}$$

The exponential on the right-hand side of Eq. (60) may be rewritten:

$$e^{-q(|z|+|z'|)}\equiv\theta(z)\theta(z')\,e^{-q(z+z')}+\theta(-z)\theta(-z')e^{q(z+z')}$$
$$+[1-\theta(z)\theta(z')-\theta(-z)\theta(-z')]e^{-q|z-z'|}\ . \tag{61}$$

Thus, choosing the normalization constant for the bulk modes,

$$\mathfrak{N}_\kappa^{(B)}(q\omega)=2\pi e^2\ , \tag{62}$$

independent of κ, q, and ω, we verify that

$$\frac{1}{2\pi e^2}\left(\int_0^\infty\frac{d\kappa}{\pi}\,\phi_\kappa^{(B)}(qz\omega)\phi_\kappa^{(B)}(qz'\omega)+\phi_\kappa^{(U)}(qz\omega)\phi_\kappa^{(U)}(qz'\omega)\right.$$
$$\left.+q\phi_0^{(S)}(qz\omega)\phi_0^{(S)}(qz'\omega)\right)=\frac{2\pi e^2}{q}\,e^{-q|z-z'|}\ , \tag{63}$$

which is the completeness condition for the ϕ's.

We are now in a position to evaluate the density-density response function [cf. Eq. (22)] which later will be used to evaluate the excitation of our model solid by an incident charged particle. We obtain

$$\int dz_1\,dz_2\,f_q(z-z_1)s_{q\omega}(z_1,z_2)f_q(z_2-z')$$
$$=\sum_l\frac{\lambda_l(q\omega)}{1-\lambda_l(q\omega)}\,\frac{\phi_l(qz\omega)\phi_l(qz'\omega)}{\mathfrak{N}_l(q\omega)}$$
$$=\frac{2\pi e^2}{q}\left(\frac{\omega_p^2}{2\omega^2-\omega_p^2}\,e^{-q(|z|+|z'|)}\right.$$
$$\left.+\frac{\omega_p^2}{\omega^2-\omega_p^2}\,\theta(z)\theta(z')(e^{-q|z-z'|}-e^{-q(z+z')})\right)\ , \tag{64}$$

which is valid at high frequencies, for the step-function electron-density profile.

In view of the correspondence between this model and the hydrodynamic theory of the semi-infinite electron gas, it is not surprising that, as shown in Sec. IV A, the expressions for energy loss by a fast electron, computed using Eq. (64), agree with those of Ritchie.[27] What at first glance may seem more surprising is that using the "semiclassical" vertex of Gersten,[46] which corresponds to taking

$$\phi_\kappa^{(B)}(qz\omega) \propto \sin\kappa z \ , \tag{65}$$

we also recover formula (64). The $\phi_\kappa^{(B)}$'s of Eqs. (55b) and (65) are obviously different. Yet each of them represents a set of functions which vanish at $z=0$ and which are complete in the half-space $z>0$. Thus, either set of $\phi_\kappa^{(B)}$ fulfills the criteria that originally were imposed following Eq. (43).

There is no paradox in these remarks. The individual $\phi_\kappa^{(B)}$ never enter the calculation of a physical quantity. Rather, what enters is the sum

$$\int \frac{d\kappa}{\pi} \frac{\lambda_\kappa^{(B)}(q\omega)}{1-\lambda_\kappa^{(B)}(q\omega)} \frac{\phi_\kappa^{(B)}(qz\omega)\phi_\kappa^{(B)}(qz'\omega)}{\mathfrak{N}_\kappa(qz\omega)} \ . \tag{66}$$

In the high-frequency approximation $\lambda_\kappa^{(B)} = \omega_p^2/\omega^2$ independent of κ, and thus all the bulk plasmons are degenerate. It is precisely for this reason that we obtain the same physical result for the two sets of $\phi^{(B)}$'s. All that enters Eq. (64) as the bulk-plasmon contribution is

$$\frac{\omega_p^2/\omega^2}{1-\omega_p^2/\omega^2} \int \frac{d\kappa}{\pi} \frac{\phi_\kappa^{(B)}(qz\omega)\phi_\kappa^{(B)}(qz'\omega)}{\mathfrak{N}_\kappa(q\omega)} \ . \tag{67}$$

Thus, if we have convinced ourselves that the surface plasmon plus the bulk plasmons constitute the complete set of modes [as we have, in fact, in the calculation leading to Eq. (63)], the result Eq. (64) may be written down directly, without any reference to the form of individual $\phi_\kappa^{(B)}$, using

$$\sum_{\text{BULK } l} \frac{\phi_l(qz\omega)\phi_l(qz'\omega)}{\mathfrak{N}_l(q\omega)} = \theta(z)\theta(z')\left(\sum_{\text{ALL } l} \frac{\phi_l(qz\omega)\phi_l(qz'\omega)}{\mathfrak{N}_l(q\omega)} - \frac{\phi_0^{(S)}(qz\omega)\phi_0^{(S)}(qz'\omega)}{\mathfrak{N}_l(q\omega)} \right)$$

$$= \theta(z)\theta(z')\frac{2\pi e^2}{q}\left(e^{-q|z-z'|} - e^{-q(z+z')}\right) \ . \tag{68}$$

However, if one should wish to construct a simple model which includes bulk-plasmon dispersion by introducing a κ dependence into the $\phi_\kappa^{(B)}(q\omega)$'s, then it will be important to choose a "good" set of $\phi^{(B)}$'s. For this purpose the set given in Eq. (55b) seems preferable to that given in Eq. (65). Note that if $\phi_\kappa^{(B)}$ is given by Eq. (65) then the corresponding density fluctuation

$$u_\kappa^{(B)}(qz\omega) = \frac{1}{4\pi e^2}\left(q^2 - \frac{d^2}{dz^2}\right)\phi_\kappa^{(B)}(qz\omega)$$

$$\propto \frac{q^2+\kappa^2}{4\pi e^2} \sin\kappa z\theta(z) + \frac{\kappa}{4\pi e^2}\delta(z) \ , \tag{69}$$

which contains a surface-charge fluctuation, that is, a term proportional to $\delta(z)$. The $\mu_\kappa^{(B)}$ corresponding to Eq. (65) do not contain a $\delta(z)$ term, which intuitively seems more reasonable for a bulk-plasma fluctuation. (A discussion of the hydrodynamic theory with dispersion is given in the Appendix.)

To conclude our study of the step-function-density model, let us take note of several of its special features:

(i) There is only one surface mode. The possibility of surface-dipole or higher-multipole resonances is not realized in this simple model.

(ii) The modes are dispersionless, and the ϕ_l are independent of frequency. Neither of these features of the model is realistic. Nevertheless they are useful in that they render various calculations simple.

(iii) The orthogonality of the bulk modes to the surface mode fixes the phase of their respective sinusoidal variations and forces $\phi_\kappa^{(B)}(z<0)=0$. The useful consequences of the orthogonality relation are less clear in more realistic models.

We now turn to a more complete, if not more realistic, model of the solid-vacuum interface, the infinite-wall model,[31] which permits the evaluation of $s_{q\omega}(z, z')$ for all values of ω, not just the high frequencies, and for which the "special features" of the step-function density model are no longer true. In particular we expect that the ϕ_l's will be frequency dependent and the corresponding λ_l's, q and ω dependent. Also, we expect there to be higher surface-multipole modes.[43]

C. Infinite-Wall Model

The infinite-wall model consists in assuming the electrons in the solid to be bound by the potential

$$V(z) = \begin{cases} 0 \ , & z>0 \\ \infty \ , & z<0 \end{cases} \tag{70}$$

rather than any self-consistent well. The kernel of the RPA equation is thus obtained from Eq. (3) by the substitution of

$$\psi_n(z) \to \psi_k(z) = \theta(z)\sin kz \ , \tag{71a}$$

$$\omega_n \to \omega_k = k^2/2m \ , \tag{71b}$$

$$\sum_n \to \int_0^\infty 2dk/\pi \ . \tag{71c}$$

The result (neglecting the electron spin) is

$$\mathcal{L}(q;\ z,\ z';\ \omega) = \int \frac{d^2k}{(2\pi)^2} \int_0^\infty \frac{2dk_1}{\pi} \int_0^\infty \frac{2dk_2}{\pi} \frac{\theta_{kk_2} - \theta_{k+qk_1}}{\omega - \omega_{k+qk_1} + \omega_{kk_2}} \sin k_1 z \sin k_1 z' \sin k_2 z \sin k_2 z'\, \theta(z)\theta(z') \ . \tag{72}$$

The fact that the integral of Eq. (72) is even in both k_1 and k_2 enables us to convert it to the useful form

$$\mathcal{L}(q;\ z,\ z';\ \omega) = \int \frac{d^2k}{(2\pi)^2} \int_{-\infty}^\infty \frac{dk_1}{2\pi} \int_{-\infty}^\infty \frac{dk_2}{2\pi} \frac{\theta_{kk_2} - \theta_{k+qk_1}}{\omega - \omega_{k+qk_1} + \omega_{kk_2}}$$

$$\times 2\cos(k_1 - k_2)z[\cos(k_1 - k_2)z' - \cos(k_1 + k_2)z']\theta(z)\theta(z') \ . \tag{73}$$

We thus obtain the RPA equation for the normal-mode charge fluctuation in the infinite-wall model [cf. Eq. (9)]:

$$\lambda(q\omega)u(qz\omega) = \int \frac{d^2k}{(2\pi)^2} \int_{-\infty}^\infty \frac{dk_1}{2\pi} \int_{-\infty}^\infty \frac{dk_2}{2\pi} \frac{\theta_{kk_2} - \theta_{k+qk_1}}{\omega - \omega_{k+qk_1} + \omega_{kk_2}} 2\cos(k_1 - k_2)z$$

$$\times \int_0^\infty dz_1 \int_0^\infty dz_2 [\cos(k_1 - k_2)z_1 - \cos(k_1 + k_2)z_1] \frac{2\pi e^2}{q} e^{-q|z_1 - z_2|} u(qz_2\omega) \ . \tag{74}$$

Following Beck,[31a] we Fourier cosine transform according to

$$u(q\kappa_\perp\omega) = 2\int_0^\infty dz \cos\kappa_\perp z\, u(qz\omega) \ , \tag{75a}$$

$$u(qz\omega) = \int_0^\infty \frac{dk_\perp}{\pi} \cos\kappa_\perp z\, u(q\kappa_\perp\omega) \ . \tag{75b}$$

Thus we obtain from Eq. (74)

$$\lambda(q\omega)u(q\kappa_\perp\omega) = 4\pi^2 e^2 \int \frac{d^2k}{(2\pi)^2} \frac{dk_1}{2\pi} \frac{dk_2}{2\pi} \frac{\theta_{kk_2} - \theta_{k+qk_1}}{\omega - \omega_{k+qk_1} + \omega_{kk_2}} [\delta(k_1 - k_2 - \kappa_\perp) + \delta(k_2 - k_1 - \kappa_\perp)]$$

$$\times \left(\frac{1}{q^2 + (k_1 - k_2)^2} [u(qk_1 - k_2\omega) - \sigma(q\omega)] - \frac{1}{q^2 + (k_1 + k_2)^2} [u(qk_1 + k_2\omega) - \sigma(q\omega)] \right) \ , \tag{76}$$

where we have defined

$$\sigma(q\omega) \equiv \int_0^\infty dz_2 e^{-qz_2} u(qz_2\omega) = \int_0^\infty \frac{dk_\perp}{\pi} \frac{q}{q^2 + \kappa_\perp^2} u(qk_\perp\omega) \ . \tag{77}$$

Carrying out the k_1 integration, and changing variables according to

$$k_2 = \tfrac{1}{2}(\kappa_\perp' - \kappa_\perp) \ , \tag{78}$$

Eq. (76) is reduced, finally, to the simple form

$$\lambda(q\omega)u(q\kappa_\perp\omega) = \frac{4\pi e^2}{q^2 + \kappa^2} L(q,\ \kappa_\perp;\ \omega)u(q\kappa_\perp\omega) - \left(\frac{4\pi e^2}{q^2 + \kappa_\perp^2} L(q,\ \kappa_\perp;\ \omega) - 2\pi e^2 \int_{-\infty}^\infty \frac{d\kappa_\perp'}{2\pi} \frac{L(q;\ \kappa_\perp,\ \kappa_\perp';\ \omega)}{q^2 + \kappa_\perp'^2} \right) \sigma(q\omega)$$

$$- 2\pi e^2 \int_{-\infty}^\infty \frac{d\kappa_\perp'}{2\pi} L(q;\ \kappa_\perp,\ \kappa_\perp';\ \omega) \frac{u(q\kappa_\perp'\omega)}{q^2 + \kappa_\perp'^2} \ , \tag{79}$$

where, following the notation of Beck,

$$L(q;\ \kappa_\perp,\ \kappa_\perp';\ \omega)\equiv\int\frac{d^2k}{(2\pi)^2}\ \frac{\theta_{k,(\kappa_\perp'-\kappa_\perp)/2}-\theta_{k+q,(\kappa_\perp'+\kappa_\perp)/2}}{\omega-\omega_{k+q,(\kappa_\perp'+\kappa_\perp)/2}+\omega_{k,(\kappa_\perp'-\kappa_\perp)/2}} \tag{80}$$

and

$$L(q,\ \kappa_\perp;\ \omega)\equiv\int_{-\infty}^{\infty}\frac{d\kappa_\perp'}{4\pi}\,L(q;\ \kappa_\perp,\ \kappa_\perp';\ \omega)\ . \tag{81}$$

Notice that the bulk (RPA) dielectric constant is directly related to $L(q,\ \kappa_\perp;\ \omega)$, according to

$$\epsilon_\infty(q,\ \kappa_\perp,\ \omega)=1-\frac{4\pi e^2}{q^2+\kappa_\perp^2}\,L(q,\ \kappa_\perp;\ \omega)\ . \tag{82}$$

The eigenvalue equation [Eq. (79)] is partially separable, in that σ is independent of $\kappa_\perp'$. There are therefore two types of solution to Eq. (79), those for which $\sigma\neq 0$, and those for which $\sigma=0$. This situation corresponds nicely to that of the step-function density that we have previously described [see, e.g., the discussion of Eq. (49)]; by definition [see, e.g., Eq. (77)],

$$\sigma(q\omega)=(q/2\pi e^2)\phi(q0\omega)\ , \tag{83}$$

where ϕ, as before, is given in terms of u by Eq. (28). Thus the criteria, σ equal or not equal to zero, are equivalent to the criteria $\phi(z=0)$ equal or not equal to zero that distinguished bulk and surface modes, respectively, in the previous model, according to the orthogonality relation.

One should take note of the physical meaning of $\sigma(q\omega)$. The expression on the right-hand side of Eq. (83) is proportional to the electric field normal to the wall at $z=0$, which, as we know from Gauss's law, yields a "surface charge." Thus the condition $\sigma\neq 0$, nonvanishing surface charge, seems appropriate for a surface oscillation.

Beck[31a] has solved Eq. (79) for the surface mode to obtain its dispersion relation. The method is as follows: Let

$$u(q\kappa_\perp\omega)\equiv\sigma(q\omega)[1-\nu(q\kappa_\perp\omega)]\ , \tag{84}$$

which is nontrivial if $\sigma\neq 0$. Substitute Eq. (84) in Eq. (79), and divide through by $\sigma(q\omega)$. Then

$$\nu(q\kappa_\perp\omega)=1\Big/\left(\lambda(q\omega)-\frac{4\pi e^2}{q^2+\kappa_\perp^2}\,L(q,\ \kappa_\perp;\ \omega)\right)$$
$$\times\left(\lambda(q\omega)-2\pi e^2\int\frac{d\kappa_\perp'}{2\pi}\,L(q;\ \kappa_\perp,\ \kappa_\perp';\ \omega)\,\frac{\nu(q\kappa_\perp'\omega)}{q^2+\kappa_\perp'^2}\right)\ . \tag{85}$$

Beck solves the inhomogeneous integral equation (85) with $\lambda(q,\ \omega)=1$. The solution, however, is only consistent with Eq. (77) if [substituting Eq. (84) in Eq. (77)]

$$1=\int_0^\infty\frac{d\kappa_\perp}{\pi}\,\frac{q}{q^2+\kappa_\perp^2}\,[1-\nu(q\kappa_\perp\omega)]\ . \tag{86}$$

Equation (86), which gives ω as a function of q, is thus the dispersion relation for the surface mode.

It is straightforward to verify that at $q=0$, Eq. (86) yields $\omega=\omega_p/\sqrt{2}$, in agreement with the result for the sharp-density-profile model, and with the general (RPA) theorem concerning the infinite-wavelength surface-plasmon frequency.[35] We notice that the factor $q/(q^2+\kappa_\perp^2)$ in Eq. (86) behaves like a δ function in $\kappa_\perp$ as $q\to 0$. We therefore examine the right-hand side of Eq. (85) in the limit $q\to 0$ with $\kappa_\perp$ taken to be of $O(q)$ (and $\lambda=1$). Referring to Eq. (25), we see that

$$L[q;\ \kappa_\perp=O(q),\ \kappa_\perp';\ \omega]=O(q^2)\ . \tag{87}$$

This implies that the second term within brackets on the right-hand side of Eq. (85) is of $O(q)$, and therefore negligible compared to $\lambda(q\omega)=1$. In the same limit, $q\to 0$, $\kappa_\perp=O(q)$,

$$\frac{4\pi e^2}{q^2+\kappa_\perp^2}\,L(q,\ \kappa_\perp;\ \omega)=\frac{\omega_p^2}{\omega^2}\ . \tag{88}$$

Therefore, in the long-wavelength limit, we may write

$$\nu(q,\ \kappa_\perp,\ \omega)=\frac{1}{1-\omega_p^2/\omega^2}\ . \tag{89}$$

Substituting Eq. (89) in Eq. (86), we see that

$$1=\frac{-\omega_p^2/\omega^2}{1-\omega_p^2/\omega^2}\int_0^\infty\frac{dk_\perp}{\pi}\,\frac{q}{q^2+\kappa_\perp^2}=-\frac{1}{2}\,\frac{\omega_p^2}{\omega^2-\omega_p^2}\ , \tag{90}$$

from which the result $\omega^2=\omega_p^2/2$ follows directly.

The fact that the integral term in Eq. (85) is $O(q)$ means that a long-wavelength expansion of ν can be easily generated by iteration. In this way a closed-form expression for the coefficient of the term linear in q in the dispersion relation can be obtained if desired.

To obtain the $u(q\kappa_\perp\omega)$ corresponding to modes other than the surface plasmon, we must solve Eq. (79) with $\sigma=0$. That is, we must find a $u(q\kappa_\perp\omega)$ which satisfies simultaneously

$$u(q\kappa_\perp\omega)=\left[-2\pi e^2\Big/\left(\lambda(q\omega)-\frac{4\pi e^2}{q^2+\kappa_\perp^2}\,L(q,\ \kappa_\perp;\ \omega)\right)\right]\int_{-\infty}^{\infty}\frac{d\kappa'}{2\pi}\,L(q;\ \kappa_\perp,\ \kappa_\perp';\ \omega)\frac{u(q\kappa_\perp'\omega)}{q^2+\kappa_\perp'^2}\ , \tag{91a}$$

$$\int_0^\infty\frac{d\kappa_\perp}{\pi}\,\frac{qu(q\kappa_\perp\omega)}{q^2+\kappa_\perp^2}=0\ . \tag{91b}$$

In general, we expect the solutions of Eq. (91a) to come in pairs (doubly degenerate solutions) corresponding to sinelike and cosinelike waves in the interior of the solid. The condition (91b) then fixes the phase of the bulk wave. This is quite analogous to the situation in the sharp-profile model, in which the orthogonality condition Eq. (49) was used to determine the phase of $u_\kappa^{(B)}(qz\omega)$, cf. Eqs. (48) and (50).

Finally, let us examine the potentials, outside the solid, associated with bulk and surface modes in the infinite-wall model. We obtain the respective ϕ's for $z<0$, using Eq. (28), and simply ignore the question of what it means to be "outside" a system bounded by an infinite potential wall. In general,

$$\phi(q\,z<0\,\omega)=\frac{2\pi e^2}{q}e^{qz}\int_0^\infty dz'\,e^{-qz'}u(qz'\omega)$$

$$=\frac{2\pi e^2}{q}e^{qz}\sigma(q\omega)\ . \qquad (92)$$

Thus the surface mode is the only one whose electric field extends outside the solid. All other modes have $\sigma=0$, and therefore $\phi(q\,z<0\,\omega)=0$.

It is possible that Eqs. (91) will have discrete surface solutions in addition to the continuum of bulk modes. These might include a surface-dipole, -tripole, or higher-multipole charge fluctuation. But according to Eqs. (91b) and (92), the potentials due to such modes could not be felt by a particle outside the solid; thus they would represent a peculiar set of surface-charge oscillations.

We conclude our discussion of the infinite-wall model by commenting on several of its special features:

(a) The RPA equation is partially separable. As a result it is easy to obtain the surface-plasmon solution.

(b) The condition, $\sigma=0$ or $\sigma\neq0$, distinguishes between bulk and surface modes. As a result only the surface mode has a nonzero potential outside the solid.

(c) The condition $\sigma=0$ for bulk modes fixes the phase shift suffered by a bulk plasmon as it reflects from the surface. This is analogous to the effect of the orthogonality condition in the step-density-profile model. It is difficult to apply orthogonality directly in the infinite-wall model (and more realistic ones) because it holds only between u_l's at the same value of ω. But surface and bulk modes oscillate at different frequencies. Thus to the extent that the u's vary with ω, the orthogonality relation is not helpful.

There are no other models, to date, which have been studied. We therefore turn our attention to the interpretation of experimental results using the model charge-mode profiles and dispersion relations.

IV. VERTEX FUNCTIONS AND THEIR APPLICATION IN ELECTRON-SOLID SCATTERING

In Sec. II we developed a microscopic description of electron-solid interactions and examined in Sec. III its consequences for simple models. In this section we first display the relation between our microscopic theory and the phenomenological inelastic-collision model of ILEED.[8,9,47–50] Then we note some of the directly observable experimental consequences in keV electron transmission of the orthogonality of the bulk- and surface-plasmon particle-hole density fluctuations.

A. Relation between Inelastic-Collision Model of ILEED and Microscopic Theory

The inelastic-collision model of inelastic electron-solid scattering was proposed by Duke and Laramore,[8] used by them to predict several qualitative features of ILEED,[9,47,48] and subsequently refined by Duke and Bagchi[49] who applied it to analyze experimental ILEED intensities from[49,50] Al(111) and Al(100).[49] In this model, the incident electron interacts with boson fields which characterize the excitation spectrum of the target solid. The combined effects of the electron-boson interaction vertex and the dynamics of the propagation of the boson are described by the loss-mode spectral density defined by Eq. (2.9) in Duke and Laramore.[8] Here we examine the coordinate representation of a closely related boson spectral density[51] $\Lambda(\vec{r}',\vec{r},i\omega_n)$, $\omega_n=2\pi n/\kappa T$ which is related to Duke and Laramore's loss-mode spectral density $[\Lambda(n,\ m,\ \omega)]$ by

$$\Lambda(n,\ m,\ \omega)=-2iN(\omega)\,\mathrm{Im}\Lambda(\vec{R}_n,\ \vec{R}_m,\ i\omega_n\to\omega+i\delta)\ , \qquad (93a)$$

$$N(\omega)=[e^{\hbar\omega/kT}-1]^{-1} \qquad (93b)$$

in which $\vec{R}_n$ and $\vec{R}_m$ designate the positions of ion-core scatterers in the target lattice.

The correspondence between our microscopic theory and the phenomenological inelastic-collision model of ILEED is obtained by comparing their respective predictions as to the form of $\Lambda(\vec{r}',\vec{r},i\omega_n)$. It is convenient to consider the case of dispersionless bulk and surface plasmons because this limit emerges naturally from applying the high-frequency expansion to analyze the step-density model (Sec. III B). The boson spectral density for this model is given by Eq. (64) to be

$$\Lambda_{SD}(\vec{r}',\ \vec{r},\ i\omega_n)=\int\frac{d^2q}{(2\pi)^2}e^{i\vec{q}\cdot(\vec{r}'-\vec{r})}\Lambda_{SD}\times(z',\ z;\ \vec{q},\ i\omega_n)\ , \qquad (94a)$$

$$\Lambda_{SD}(z',\ z;\ \vec{q},\ i\omega_n)=\Lambda_{sp}(z',\ z,\ q;\ i\omega_n)+\Lambda_{op}(z',\ z,\ q;\ i\omega_n)\ , \qquad (94b)$$

$$\Lambda_{sp}(z',\ z;\ \vec{q},\ i\omega_n)=\frac{2\pi e^2}{q}\ \frac{-(\omega_p^2/2\omega_n^2)}{1+(\omega_p^2/2\omega_n^2)}\ e^{-q(|z|+|z'|)}\ , \tag{94c}$$

$$\Lambda_{bp}(z',\ z;\ q;\ i\omega_n)=\frac{2\pi e^2}{q}\ \frac{-\omega_p^2/\omega_n^2}{1+(\omega_p/\omega_n)^2}\ \theta(z)\theta(z') \times(e^{-q|z-z'|}-e^{-q(z+z')})\ . \tag{94d}$$

In the case of surface plasmons characterized by the dispersion relation

$$\hbar\omega_s(q)=\hbar\omega_s=\hbar\omega_p/\sqrt{2}\ , \tag{95}$$

Eqs. (2.10) and (2.18) in Duke and Laramore[8] give

$$\Lambda_{sp}(z',z;\vec{q},i\omega_n)=\frac{\pi e^2\hbar\omega_s}{q}\left(\frac{1}{i\hbar\omega_n-\hbar\omega_s}-\frac{1}{i\hbar\omega_n+\hbar\omega_s}\right) \times e^{-q(|z'|+|z|)}\ , \tag{96}$$

which is identical to Eq. (94c). Thus the phenomenological model of Duke and Laramore, describing the semiclassical electrostatic coupling of the incident electron to dispersionless surface-plasmon modes, is identical to the predictions of microscopic theory for the leading term of the high-frequency expansion of the RPA applied to a step-density model.

Turning to the case of the incoherent coupling of the incident electron to bulk plasmons as described by Duke and Laramore, from Eqs. (2.10) and (2.15) of their paper,[8] we obtain

$$\Lambda_{ibp}(z',z;q,i\omega_n)=\int_{-p_c}^{p_c}\frac{dp_\perp}{2\pi}\ \frac{2\pi e^2\hbar\omega_p}{p_\perp^2+q^2}\ e^{ip_\perp(z'-z)} \times\frac{1}{i\hbar\omega_n-\hbar\omega_b(p_\perp,q)}-\frac{1}{i\hbar\omega_n+\hbar\omega_b(p_\perp,q)}\ . \tag{97a}$$

If we formally extend the cutoff momentum[52] p_c to infinity, we obtain for dispersionless bulk plasmons $[\hbar\omega_b(p)=\hbar\omega_p)]$

$$\Lambda_{ibp}(z',z;\vec{q},i\omega_n)=\frac{2\pi e^2}{p}\ \frac{[-(\omega_p/\omega_n)^2]}{1+(\omega_p/\omega_n)^2}\ e^{-q|z-z'|}\ . \tag{97b}$$

Thus only the "bulk" term in Eq. (94d) involving $|z-z'|$ is predicted by the incoherent-coupling model vertex. In addition, the extension of the integration limits to infinity implies $q\ll p_c\sim 1$ Å^{-1}. Finally, it is evident from the analysis leading to Eq. (64) that the use of Eqs. (97) for the electron-plasmon vertex involves "double counting" of the effects of surface plasmons. That is, the $e^{-q|z-z'|}$ factor in Eq. (97b) results from the completeness condition Eq. (63) alone, whereas in Eq. (64) the correct weighting of the bulk-plasmon terms is obtained by subtracting from the total $e^{-q|z-z'|}$ factor the factor $e^{-q(|z|+|z'|)}$ due to surface plasmons and an appropriate factor for the "unobservable" plasmon modes with $\lambda\equiv 0$, which are localized outside the crystal.

Duke and Laramore recognized the difficulties inherent in the use of Eqs. (97) and sought to remedy them by using sine-wave plasmon-basis states which vanished outside the sample. The electron interaction with these states was taken to be the semiclassical form derived by Gersten.[46] The phase-space weighting of these modes is given by

$$\sum_p\rightarrow c\int_0^{p_c}dp/\pi\ . \tag{98}$$

From the normalization Eq. (52) we would expect $c=2$. However, because the solid only occupies one-half the normalization volume, we take $c=1$. Using this choice in Eqs. (2.10) and (2.18) of Duke and Laramore[8] gives

$$\Lambda_{cbp}(z',z;\vec{q},i\omega_n)=\int_0^{p_c}\frac{dp_\perp}{p_\perp^2+q^2}\ \frac{4e^2\hbar\omega_p}{} \times\left(\frac{1}{i\hbar\omega_n-\hbar\omega_b(p_\perp,q)}-\frac{1}{i\hbar\omega_n-\hbar\omega_b(p_\perp,q)}\right) \times\theta(z)\theta(z')\sin(p_\perp z)\sin(p_\perp z')\ . \tag{99a}$$

In the limit that $\hbar\omega_b(p)=\hbar\omega_p$ and $q\ll p_c$, we obtain from Eq. (99a)

$$\Lambda_{cbp}(z',z;\vec{q},i\omega_n)=\frac{2\pi e^2}{q}\ \frac{-(\omega_p/\omega_n)^2}{1+(\omega_p/\omega_n)^2}\ \theta(z)\,\theta(z') \times(e^{-q|z-z'|}-e^{-q(z+z')})\ , \tag{99b}$$

which is precisely the result Eq. (94d) given by the step-density model in the high-frequency limit of the RPA. Therefore, the coherent-coupling model of Duke and Laramore correctly accounts for the consequences of the orthogonality and completeness of the bulk- and surface-plasmon density fluctuations in the limit that $\hbar\omega_b(p)\rightarrow\hbar\omega_p$. The theory developed in Sec. III suggests that when plasmon dispersion and damping are considered, the semiclassical coherent-coupling vertex is accurate only in the $q\rightarrow 0$ limit. However, the major modification of the simple RPA required by the analysis of experimental data[49,50] is the abandonment of plane-wave basis states for motion parallel to the surface. Therefore no consideration of vertex renormalization using plane-wave models has been attempted.

B. Experimental Consequences of Completeness and Orthogonality: Inelastic-Electron Transmission through Thin Films

In Sec. IV A we found that the orthogonality and completeness of the bulk- and surface-density fluctuations resulted in a modification of the electron-bulk-plasmon spectral density relative to its form for an "infinite" medium. The consequences for ILEED of this "vertex" modification were examined by Laramore and Duke.[8] Unfortunately, however, the damping of the bulk plasmons renders

unobservable, in any practical sense, the predicted effects in ILEED experiments.[9,49] Therefore, in this section we turn to an examination of keV electron-transmission experiments in order to demonstrate the experimental observation of the consequences of the completeness relations for density fluctuations.

The measurements which we consider are those of the angular distribution of inelastically transmitted keV electrons of incident wave vector $k=(2mE/\hbar^2)^{1/2}$ from films sufficiently thin that $kd\lesssim 1$. The symbol d designates the thickness of the presumed uniform planar film. For convenience we restrict our attention to normal incidence (i.e., $\vec{k}_{\parallel}=0$, $k_{\perp}=k$). We shall find that the completeness relations manifest themselves in the reduction of the forward-scattering bulk-plasmon-emission cross section. This phenomenon has been observed for some time.[26,53-55] It has been interpreted[55] in terms of the "boundary corrections" originally predicted by Ritchie using the hydrodynamic model.[27,56] As expected from the general analysis in Sec. III, our results for the high-frequency limit of the RPA applied to the step-density model are identical with those of Ritchie. Therefore we are able to show that the electron-plasmon-vertex modifications predicted by our microscopic theory lead, in the appropriate limits, to the hydrodynamic description of an observed phenomenon.

The first step in our analysis is the specification of the density fluctuations $u_l(qz\omega)$ for a film of thickness d analogous to those given by Eqs. (54) for the semi-infinite medium. Taking the center of the slab to be at $z=0$, we use

$$u_{\pm}^{(S)}(qz\omega)=2^{-1/2}[\delta(z+\tfrac{1}{2}d)\pm\delta(z-\tfrac{1}{2}d)], \tag{100a}$$

$$u_{ak}^{(B)}(qz\omega)=\sin k_a z\,\theta(z+\tfrac{1}{2}d)\,\theta(\tfrac{1}{2}d-z), \tag{100b}$$

$$u_{sk}^{(B)}(qz\omega)=\cos k_s z\,\theta(z+\tfrac{1}{2}d)\,\theta(\tfrac{1}{2}d-z). \tag{100c}$$

The orthogonality of the bulk- and surface-density fluctuations, i.e., Eq. (44), leads either to identities or to eigenvalue conditions on k_a and k_s. The normalization integrals for the surface-plasmon modes are given by

$$\mathfrak{N}_{\pm}^{(S)}(q\omega)=\frac{2\pi e^2}{q}(1\pm e^{-qd}), \tag{101}$$

in contrast to Eq. (59) for the semi-infinite medium.

The quantity which we wish to calculate is the spectral density for the emission of dispersionless bulk plasmons $\hbar\omega_b(p)\equiv\hbar\omega_p$. From Eq. (64) we obtain

$$\Lambda_{bp}(z,z';\vec{q},i\omega_n)=-\frac{(\omega_p/\omega_n)^2}{1+(\omega_p/\omega_n)^2}F_q^{(B)}(z,z'), \tag{102a}$$

$$F_q^{(B)}(z,z')=\theta(z+\tfrac{1}{2}d)\,\theta(z'+\tfrac{1}{2}d)\,\theta(\tfrac{1}{2}d-z')\theta(\tfrac{1}{2}d-z)$$
$$\times\left(\frac{2\pi e^2}{q}e^{-q|z-z'|}-\frac{\phi_-^{(S)}(z)\,\phi_-^{(S)}(z')}{\mathfrak{N}_-^{(S)}}-\frac{\phi_+^{(S)}(z)\,\phi_+^{(S)}(z')}{\mathfrak{N}_+^{(S)}}\right). \tag{102b}$$

The $\phi_{\pm}^{(S)}(z)$ are calculated from Eqs. (28) and (100). When they are inserted in Eq. (102b) and the origin ($z=0$) is changed to the left-hand edge of the film, we obtain

$$F_q^{(B)}(z,z')=\frac{2\pi e^2}{q}\,\theta(z)\,\theta(z')\,\theta(d-z)\,\theta(d-z')$$
$$\times\{e^{-q|z-z'|}-(1-e^{-2qd})^{-1}[e^{-q(z+z')}+e^{-q(2d-z-z')}$$
$$-e^{-q(2d+z-z')}-e^{-q(2d-z-z')}]\}. \tag{103}$$

Inserting Eq. (103) into (102a) completely specifies the bulk-plasmon spectral density.

The Born approximation for the inelastic-scattering cross section for bulk-plasmon emission (by forward scattering) from $\vec{k}=(0,k)$ to $\vec{k}'=(\vec{q},k_{\perp}')$ with loss energy w is given by

$$\frac{d2\sigma}{d\epsilon\,d\Omega}=-\frac{2mA}{\hbar^2k}\int\frac{k'^2\,dk'}{(2\pi)^3}\,\delta\left(w-\frac{\hbar^2k'^2}{2m}+\frac{\hbar^2k^2}{2m}\right)$$
$$\times\int_0^d dz\int_0^d dz'\,e^{-i(k_{\perp}'-k)(z-z')}\,\mathrm{Im}\Lambda_{bp}(z,z';\vec{q},i\hbar\omega_n\to\omega+i\delta), \tag{104}$$

in which A is the surface area of the film. Noting that for plasmon emission Eq. (102a) gives

$$\mathrm{Im}\Lambda_{bp}(z,z';\vec{q},i\hbar\omega_n\to w+i\delta)=-\tfrac{1}{2}\pi\hbar\omega_p\,\delta(w-\hbar\omega_p)$$
$$\times F_q^{(B)}(z,z'), \tag{105}$$

we obtain our final result

$$\frac{d^2\sigma}{dE\,d\Omega}=\frac{dA}{2\pi a_B}\,\delta(w-\hbar\omega_p)\left[\frac{\theta_E}{\theta^2+\theta_E^2}-\frac{2}{(kd)}\frac{\theta\,\theta_E}{\theta^2+\theta_E^2}\right.$$
$$\left.\times\left(1+\frac{e^{-2kd\theta}-e^{-kd\theta}\cos(kd\theta_E)}{2(1-e^{-2kd\theta})}\right)\right], \tag{106a}$$

$$\theta=\frac{q}{k},\qquad \theta_E=\frac{k-k_{\perp}'}{k}=\frac{\hbar\omega_p}{2E}, \tag{106b}$$

in which E is the energy of the normally incident electron, θ is its scattering angle, and a_B is the Bohr radius, $a_B=\hbar^2/me^2$.

The predictions of Eqs. (106) and their comparison with the data of Kunz[53] are shown in Fig. 2. The completeness relation introduces corrections to the bulk cross section which reduce the forward-scattering inelastic cross sections in agreement with the data. The result for the bulk cross section, originally obtained by Ferrell,[57] is recovered from Eq. (106a) in the $d\to\infty$ limit. Equations (106) and Fig. 2 constitute our demonstra-

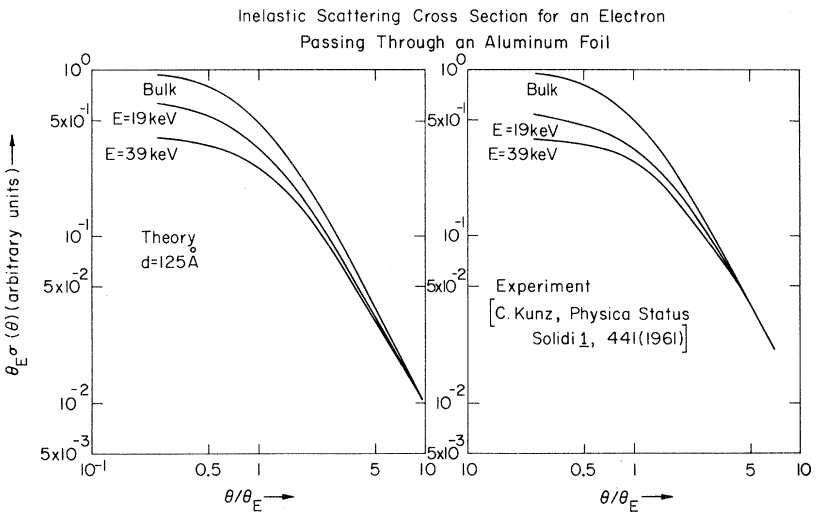

FIG. 2. Comparison of the theoretical [Eqs. (106) in the text] and experimental curves for the inelastic cross section of an electron incident normally on an aluminum foil and deflected through an angle θ with the excitation of a bulk plasmon. Curves marked "Bulk" are drawn for Ferrell's calculation of bulk plasmons in an infinite medium. Surface corrections in a finite film decreases the scattering cross section in the forward direction. The theoretical curves have been computed for a film of thickness 125 Å and for electrons with incident energies of 19 and 39 keV.

tion that the completeness relations for the density fluctuations, which lead to the "coherent-coupling" model in Duke and Laramore's theory of ILEED,[8] also lead to a directly observable experimental phenomenon. Finally, comparison of Eqs. (106) with Eq. (23) in Ritchie's paper[27] reveals, after some algebra, that in the absence of plasmon dispersion the step-density model does indeed reproduce the results of the hydrodynamic model.

V. ELECTRON-SOLID INTERACTION: EFFECTIVE OPTICAL POTENTIAL

A. Formal Scattering Theory

As emphasized in Sec. I, our main objective in this paper is the development of a microscopic theory of electron-solid scattering which incorporates the long-range and dissipative components of the force law as well as the short-range electron–ion-core interactions. We apply this theory to calculate the elastic electron-solid cross sections by proceeding in two steps. First we examine the scattering of an incident electron by semi-infinite jellium (i.e., a system in which the actual ion-core charge densities are replaced by a uniform positive background). The appropriate electronic propagators $G_0(\vec{r},\vec{r}',E)$ are evaluated using the optical-potential method of Bell and Squires.[58,41] These propagators subsequently are used in a distorted-wave multiple-scattering analysis of the electron's interactions with the short-range potential due to ion-core potentials. In this paper, however, we concentrate on the first step. The second is examined only in the distorted-wave Born approximation[59] using a highly simplified model.

The electronic propagator $G_0(\vec{r},\vec{r}',E)$ associated with the distorted-wave basis satisfies the integral equation[58,60]

$$G_0(\vec{r},\vec{r}',E) = G_{00}(\vec{r},\vec{r}',E) + \int d^3r_1\, d^3r_2\; G_{00}(\vec{r},\vec{r}_1,E) \times \Sigma(\vec{r}_1,\vec{r}_2,E)\, G_0(\vec{r}_2,\vec{r}',E)\,, \quad (107)$$

$$\left(E - \frac{\hbar^2\nabla^2}{2m}\right) G_{00}(\vec{r},\vec{r}',E) - \int d^3r_1\; V_0(\vec{r},\vec{r}_1)\, G_{00}(\vec{r}_1,\vec{r}',E) = \delta(\vec{r}-\vec{r}')\,, \quad (108)$$

in which $\Sigma(\vec{r}',\vec{r},E)$ is the retarded proper self-energy due to electron-electron interactions[60] and $V_0(\vec{r},\vec{r}')$ is any prescribed static potential. In principle, $V_0(\vec{r},\vec{r}')$ is taken to be the Hartree and Hartree-Fock contributions to $\Sigma(\vec{r},\vec{r}',E)$, although in practice such a choice is not feasible.[61] The complete propagator of the system, $G(\vec{r},\vec{r}',E)$, satisfies the integral equation

$$G(\vec{r},\vec{r}',E) = G_0(\vec{r},\vec{r}',E) + \int d^3r_1\, d^3r_2\, G_0(\vec{r},\vec{r}_1,E) \times V_L(\vec{r}_1,\vec{r}_2)\, G(\vec{r}_2,\vec{r}',E)\,, \quad (109)$$

in which $V_L(\vec{r},\vec{r}')$ is the change in potential caused by decomposing the uniform positive "jellium" background into positive ions of the appropriate charge and position. A multiple-scattering analysis[8] of Eq. (109) can be performed if $V_L(\vec{r},\vec{r}')$ is of the form

$$V_L(\vec{r},\vec{r}') = \delta(\vec{r}-\vec{r}')\textstyle\sum_n v(\vec{r}-\vec{R}_n)\,. \quad (110)$$

The elastic electron-solid cross section is obtained by examining the asymptotic form of

$$\psi_{\rm scatt}(\vec{r},E) - \phi_k(\vec{r}) = \int d^3r_1\, d^3r_2\, G(\vec{r},\vec{r}_1,E) \times V_L(\vec{r}_1,\vec{r}_2)\,\phi_k(\vec{r}_2)\,, \quad (111a)$$

$$\phi_k(\vec{r}) = e^{i\vec{k}\cdot\vec{r}} + \int d^3r_1\, d^3r_2\; G_{00}(\vec{r},\vec{r}_1,E)$$

$$\times \Sigma(\vec{r}_1, \vec{r}_2, E)\, \phi_k(\vec{r}_2)\,, \qquad (111b)$$

in which $\vec{k}$ is the wave vector of the incident electron. Therefore, in this formulation of the calculation of the elastic electron-solid cross section all effects of both the induced charge on the solid's surface and the inelastic loss processes are described by the coordinate representation of the electronic proper self-energy $\Sigma(\vec{r}, \vec{r}', E)$ for semi-infinite jellium.

The electronic proper self-energy may be evaluated readily using the formalism developed in Secs. II and III. Although a complete quantum-field theory can be constructed,[8] we confine our consideration to the linear-response expression for $\Sigma(\vec{r}, \vec{r}', E)$ as given by taking $i\hbar\omega_n \to E + i\delta$ in

$$\Sigma(\vec{r}, \vec{r}', i\omega_n) = \sum_m \Lambda(\vec{r}, \vec{r}', i\omega_m) \times G_0(\vec{r}', \vec{r},\ i\omega_n + i\omega_m)\,, \qquad (112)$$

in which Λ is the particle-hole spectral density defined and evaluated in Sec. IV A. Equation (112) reveals the significance for the calculation of the electron-solid optical potential $\Sigma(\vec{r}, \vec{r}', E)$ of the orthogonality and completeness relations of the density fluctuations u_l developed in Sec. II. By using a systematic microscopic description of these density fluctuations, we can isolate the individual contributions to the electron-solid force of surface plasmons, bulk plasmons, and bulk particle-hole pairs. This separation permits the investigation of their distinctive dependences on the position and energy variables. Therefore we can provide a physical interpretation of the range, energy dependence, and dissipative character of their respective contributions to the electron-solid optical potential. The orthogonality and completeness relations guarantee that our decomposition of the optical potential into its separate components is well defined, is unique within the framework of a given model, and incorporates all possible contributions to the potential. This decomposition leads to interesting physical results like the fact that the z^{-1} "image-force" potential outside the jellium surface is caused by virtual surface-plasmon emission, whereas inside the solid the corresponding contributions to the optical potential are canceled by virtual bulk-plasmon emission processes.

As our final preliminary to evaluating the optical potential and electron propagator, we recall that the translational symmetry parallel to the planar surface renders Eqs. (107) and (108) diagonal in the momentum variable $\vec{k}_\parallel$, for electronic motion parallel to the surface. Therefore we only need to evaluate $\Sigma(z, z', \vec{k}_\parallel, i\omega_n)$ defined by

$$(2\pi)^2\, \delta(\vec{k}_\parallel' - \vec{k}_\parallel)\ \Sigma(z, z'; \vec{k}_\parallel, i\omega_n) \equiv \int d^2\rho\, e^{-i\vec{k}_\parallel \cdot \vec{\rho}} \int d^2\rho'\, e^{i\vec{k}_\parallel \cdot \vec{\rho}'} \times \Sigma(\vec{r}, \vec{r}', i\omega_n)\,, \qquad (113a)$$

$$\Sigma(z, z'; \vec{k}_\parallel, i\omega_n) = \int \frac{d^2q}{(2\pi)^2} \sum_{i\omega_m} \Lambda(z, z'; \vec{q}, i\omega_m) \times G_0(z', z, \vec{k}_\parallel + \vec{q}, i\omega_n + i\omega_m)\,. \qquad (113b)$$

In practice, we make the additional approximation of replacing G_0 by G_{00} in Eq. (113b), i.e., using the second-order-perturbation-theory expression for the optical potential. Performing the Matsubara sum over $i\omega_m$ gives

$$\Sigma(z, z'; \vec{k}_\parallel, E) = \Sigma_{ph}(z, z'; \vec{k}_\parallel, E) + \Sigma_e(z, z'; \vec{k}_\parallel, E)\,, \qquad (114a)$$

$$\Sigma_{ph}(z, z'; \vec{k}_\parallel, E) = \int_{-\infty}^{\infty} \frac{N(x)}{\pi}\, dx \int \frac{d^2q}{(2\pi)^2} \times G_0(z, z', \vec{k}_\parallel + \vec{q}, E + x)\, \mathrm{Im}\Lambda(z, z'; \vec{q}, x), \qquad (114b)$$

$$\Sigma_e(z, z'; \vec{k}_\parallel, E) = \int_{-\infty}^{\infty} \frac{f(x)\, dx}{\pi} \int \frac{d^2q}{(2\pi)^2}\ \Lambda(z, z'; \vec{q}, E + x) \times \mathrm{Im}G_0(z, z'; \vec{k} - \vec{q}, x)\,, \qquad (114c)$$

$$f(x) = (e^{x/\kappa T} + 1)^{-1}\,. \qquad (114d)$$

For most incident electrons, $E \gtrsim 25$ eV, the exclusion-principle contribution Σ_e is small or zero. Therefore we neglect it and use Eq. (114b) as our basic formula for the electron-solid optical potential.

B. Classification of Models of Optical Potential

In the remainder of this article, we shall be evaluating the electron-solid optical potential and studying its consequences in model calculations. A logical preliminary, then, is the classification of previous models of the potential felt by a charged particle in the presence of a solid surface and a discussion of their relation to the exact equations (114).

The two principal criteria which we use to distinguish among the various models are (i) whether the motion of the external particle is completely prescribed, or is defined only insofar as initial conditions are stated; (ii) whether the motion of the external particle is restricted to be at high speed ($v \gg v_F$) or low speed ($v \lesssim v_F$) compared to the Fermi velocity v_F.

Many of the calculations in the literature of the potential seen by a charged particle outside a solid surface[21,22,62-64] are based on the assumption that the particle is a point charge, at rest, at a fixed distance from the surface. Others[65,66] assume it to be moving with constant velocity along a prescribed path. In either case, the charge induced in the solid by the particle is evaluated, and the potential due

to the induced charge is identified as the interaction of the particle with the solid.

However, the instantaneous specification of both the position and velocity of a finite-mass particle is not possible quantum mechanically; the complete specification of the trajectory of such a particle without foreknowledge of the potential it sees is not even possible classically. Models which are based on such specifications cannot be derived from exact many-body equations of motion, except in the limit that the external particle has infinite mass (see Sec. V D, below). The reliability of these models is, therefore, difficult to assess.

Only two calculations, to date, have avoided the complete specification of the external particle's trajectory, that of Gersten,[67] which is discussed below (Sec. V D), and the present one. In our model calculations, only the conserved quantum numbers (initial conditions) of the external particle are specified. That is, we fix its total energy and momentum parallel to the surface, but not its position or momentum perpendicular to the surface. Our treatment of the external particle is thus completely quantum mechanical, at the cost, however, of the introduction of nonlocality into the effective potential that influences the particle's motion.

The question of the speed of the external particle is important in that it determines the frequency at which the solid is excited, and consequently the nature of the elementary excitations of the solid to which the external particle couples. If the speed of the external particle is high ($v \gg v_F$) the excitations to which it couples are plasmons. If the speed is low ($v \lesssim v_F$) they are noncollective particle-hole states. The distinction between the two regimes arises from the fact that a particle located at a distance z from the surface moving with instantaneous speed v excites the solid at a frequency $\sim v/z$ with wave vectors whose magnitude is $\sim 1/z$. However, the dielectric response of the solid is associated with plasmons when $\omega/|\vec{k}| \gg v_F$, ω and $\vec{k}$ being the frequency and wave vector of excitation, and with particle-hole states if $\omega/|\vec{k}| \lesssim v_F$.

In the model calculations presented below, as well as in the papers of Takimoto[65] and Lucas and Sunjić,[66] use of the high-frequency approximation to the dielectric response of the solid limits the validity of the results to high-velocity external particles. Lucas[68] applies the high-frequency dielectric function in the study of plasmon excitation by ions in field ionization. Because the ions are of low velocity, this application is incorrect. We wish to apply this dielectric function in the analysis of low-energy electron diffraction, however. For incident electrons of energy $\gtrsim 10$ eV the criterion $v > v_F$ is satisfied.

Other calculations[21,22,62-64] in the literature have been performed for a static external particle. They differ in their treatment of the solid's zero-frequency response. Approximations to the dielectric function at $\omega = 0$ that have been used in recent work include the Fermi-Thomas approximation,[21,64] the infinite-wall RPA without "quantum-interference terms,"[22] and the infinite-wall RPA with "quantum-interference terms" included.[21,22] None of these calculations is directly relevant for an analysis of electron diffraction because for these electrons $v > v_F$.

C. Local-Complex-Potential Model of ELEED

In many recent model calculations of ELEED intensities[2,4-6] a local complex potential is employed to simulate the consequences of the electron-electron interactions on electron-solid scattering. Thus it is of interest to specify this model and derive some of its more important consequences within our distorted-wave scattering theory.

The local-complex-potential model is defined by specifying, *a priori*, the retarded proper self-energy $\Sigma(\vec{r}, \vec{r}', E)$ to be of the form

$$\Sigma(\vec{r}, \vec{r}', E) \equiv \delta(\vec{r} - \vec{r}')\Sigma(\vec{r}, E) . \tag{115a}$$

In practice[2,4-6] the further assumption is made that

$$\Sigma(\vec{r}, E) = V(E)\theta(z) , \tag{115b}$$

in which $V(E)$ (or at least its imaginary part) is taken to be the energy-shell one-electron self-energy in bulk jellium.[2-6,15]

Although it cannot be derived from our microscopic theory in any well-defined limit, the local-complex-potential model exhibits the interesting feature that the distorted-wave basis states, $\phi_k(\vec{r})$, defined by Eq. (111b), and propagator $G_0(\vec{r}, \vec{r}', E)$, defined by Eq. (108), can be evaluated in closed form. We find

$$G_0(z, z'; \vec{k}_{\parallel}, E) = -2mi \begin{cases} \dfrac{1}{2k_\perp}\left[e^{ik_\perp|z-z'|} - \left(\dfrac{\tilde{k}_\perp - k_\perp}{\tilde{k}_\perp + k_\perp}\right) e^{ik_\perp(z+z')}\right]; & z, z' < 0 \\ e^{-i(k_\perp z - \tilde{k}_\perp z')}/(k_\perp + \tilde{k}_\perp); & z < 0 < z' \\ e^{i(\tilde{k}_\perp z - k_\perp z')}/(k_\perp + \tilde{k}_\perp); & z' < 0 < z \\ \dfrac{1}{2\tilde{k}_\perp}\left[e^{i\tilde{k}_\perp|z-z'|} + \left(\dfrac{\tilde{k}_\perp - k_\perp}{\tilde{k}_\perp + k_\perp}\right) e^{i\tilde{k}_\perp(z+z')}\right]; & 0 < z, z' \end{cases} \tag{116a}$$

$$k_\perp^2(\vec{g}, E) = (2mE/\hbar^2) - (\vec{k}_\parallel + \vec{g})^2 , \quad (116b)$$

$$\tilde{k}_\perp^2(\vec{g}, E) = \{2m[E + V(E)]/\hbar^2\} - (\vec{k}_\parallel + \vec{g})^2 , \quad (116c)$$

in which $\vec{g}$ is a reciprocal-lattice vector of the lattice-potential layers parallel to the surface, and

$$\phi_k(\vec{r}) = e^{i\vec{k}_\parallel \cdot \vec{\rho}}\, \phi_k(z) , \quad (117a)$$

$$\phi_k(z) = \begin{cases} e^{ik_\perp z} + \left(\dfrac{k_\perp - \tilde{k}_\perp}{k_\perp + \tilde{k}_\perp}\right) e^{-ik_\perp z}; & z < 0 \\ 2k_\perp e^{i\tilde{k}_\perp z}/(k_\perp + \tilde{k}_\perp); & z > 0 \end{cases} . \quad (117b)$$

By use of Eqs. (116) and (117) in the formal scattering theory, Eqs. (109) and (111), we can illustrate the type of effects predicted by the distorted-wave scattering theory For simplicity, we consider only the distorted-wave Born approximation and use the δ-potential model of the lattice potential

$$v(\vec{r} - \vec{R}_n) = v_n\, \delta(\vec{r} - \vec{R}_n) . \quad (118)$$

After some algebra we obtain for the asymptotic form of the wave function [using Eqs. (116) and (117) in Eq. (111a)]

$$\psi_{\text{scatt}}(\vec{r}) \xrightarrow[z \to -\infty]{} e^{i\vec{k}_\parallel \cdot \vec{\rho}}\, \psi_k(z) , \quad (119a)$$

$$\psi_k(z) = R(0, E) + \sum_{\vec{g}, n} \frac{S(0, E)\, S(\vec{g}, E)\, miv_n \exp\{i[k_\perp(\vec{g}, E) + \tilde{k}_\perp(\vec{g}, E)]R_n\}}{\hbar^2 k_\perp(\vec{g}, E)} . \quad (119b)$$

The first term in Eq. (119b), i.e.,

$$R(0, E) \equiv [k_\perp(0, E) - \tilde{k}_\perp(0, E)]/[k_\perp(0, E) + \tilde{k}_\perp(0, E)] , \quad (120a)$$

gives the contribution to the scattered wave from the jellium-vacuum surface alone. The second term in Eq. (119b) is the result obtained from the Born approximation of scattering from the lattice potential, Eq. (118), alone multiplied by the product of

$$S(\vec{g}, E) \equiv 2k_\perp(\vec{g}, E)/[k_\perp(\vec{g}, E) + \tilde{k}_\perp(\vec{g}, E)] \quad (120b)$$

for the incident ($\vec{g} \equiv 0$) and final beams, i.e., the product of the transmission coefficients of jellium-vacuum interface in the absence of the lattice potential.

We have presented the results of these elementary calculations to illustrate three important features of the distorted-wave scattering theory. First, the spatial dependence of the optical potential at a solid-vacuum interface not only contributes its own reflection coefficient $R(0, E)$ to the total electron-solid cross section but also influences the electron's scattering from the short-range electron-ion-core potential. The latter influence is always strong for glancing initial or final beams, independent of the energy of the electrons. This fact has the important consequence that the ratios of the absolute intensities of different beams predicted by a model potential will depend (sensitively) on the spatial dependence and magnitude of $\Sigma(\vec{r}, \vec{r}', E)$. Second, as $\Sigma(\vec{r}, \vec{r}E)$ diminishes as E increases,[2] the extent of the dependence of the relative beam intensities on the shape of the optical potential diminishes with increasing energy of the incident electron. For more general models of the optical potential than Eqs. (115), the magnitude of the "apparent" real part of $V(E)$ depends on the beam index $\vec{g}$ as well as E so that the energies as well as the intensities of maxima in the intensity-vs-energy profiles depend on the shape of the optical potential. Third and finally, we see that $G_0(\vec{r}, \vec{r}', E)$ does not depend solely on $\vec{R} = \vec{r} - \vec{r}'$. Therefore simple multiple-scattering theories[2,69] no longer suffice to solve Eq. (109), and more general planar-scattering theories[4] must be used for this task. In this paper we do not attempt to solve this equation, but rather turn in subsequent sections to the determination of the optical potential $\Sigma(\vec{r}, \vec{r}', E)$ itself.

D. General Features of Electron-Solid Optical Potential: High-Frequency Step-Density Model

In this section we apply our microscopic description of electron-solid interactions to evaluate the electron-jellium optical potential in the simplest case: the high-frequency step-density model described in Sec. III B. Before proceeding, two general observations seem appropriate. First, we demonstrated in Sec. IV A that the electron-density-fluctuation spectral density predicted by this model is identical to that obtained using Gersten's model.[46] Using Ferrell's semiclassical analysis Gersten also applied this analysis to obtain an expression for the electron-solid optical potential of the form[46,67]

$$\Sigma_G(z, z'; \vec{k}_\parallel E) = \delta(z - z')\,[\beta(\vec{k}_\parallel, E)\, \delta(z) + \alpha(\vec{k}_\parallel, E)\, \theta(z)] . \quad (121)$$

The δ-function term is associated with surface-plasmon creation by the incident electron and the θ-function term with bulk-plasmon creation. Although detailed numerical calculations have been performed using this model,[67] the functional form of the potential was determined solely by inspection of the normalization criteria in the semiclassical analysis.[46] Our microscopic quantum description predicts drastically different spatial dependences (e.g., long-range highly nonlocal real and imaginary parts) of the optical potential from those given in Eq. (121). Thus, whereas within the high-

frequency approximation the semiclassical analysis proved adequate for evaluating electron-density-fluctuation spectral densities, it is inadequate for calculating the optical potential. Our second observation concerns the validity of the high-frequency step-density model itself. From Eq. (64) we found that in this model, $\lambda_l(q\omega)=\lambda_l(\omega)$, i.e., the bulk and surface plasmons exhibit no dispersion. Such a model is adequate only for values of ω such that $\omega \gtrsim q v_F$, where v_F denotes the Fermi velocity in jellium. This restriction on the validity of the high-frequency approximation renders this approximation inappropriate to describe the optical potential for slow electrons $[(2E/m)^{1/2}=v<v_F]$.

From Eqs. (94), (107), (108), and (114) we see that within the high-frequency step-density model the optical potential can be written as the sum of three terms,

$$\Sigma(z,z';\vec{k}_{\parallel},E)=\Sigma_{HF}(z,z';\vec{k}_{\parallel})+\Sigma_{sp}(z,z';\vec{k}_{\parallel},E)+\Sigma_{bp}(z,z';\vec{k}_{\parallel},E). \quad (122)$$

The leading term, Σ_{HF}, designates the Hartree-Fock contribution. Its range near the surface and nonlocality are both of the order of $k_F=(3\pi^2 n)^{1/3}$ for semi-infinite jellium of density n cm^{-3}. Its depth is approximately $\Sigma_{HF}\sim(\phi+\hbar^2k_F^2/2m)$ in which ϕ is the work function of the jellium system, $\phi\sim 2$–6 eV.[61] For electrons for which $k=(2mE/\hbar^2)\gg k_F$ (i.e., $E\gtrsim 100$ eV) we argue that this contribution to the optical potential is small. Therefore for the purpose of estimating this potential, we use a plane-wave basis for G_{00} in Eq. (108), rather than

$$V_0(z,z';\vec{k}_{\parallel})=\Sigma_{HF}(z,z',\vec{k}_{\parallel}),$$

i.e.,

$$G_{00}(z,z';\vec{k}_{\parallel},E)=-\int_{-\infty}^{\infty}\frac{dk}{2\pi}\,\frac{e^{ik_{\perp}(z-z')}}{(\hbar^2/2m)(k_{\perp}^2+k_{\parallel}^2)-E}=-\frac{mi}{\hbar^2\gamma}\,e^{i\gamma|z-z'|}, \quad (123a)$$

$$\gamma(E,\vec{k}_{\parallel})=[(2mE/\hbar^2)-k_{\parallel}^2]^{1/2};\quad E>\hbar^2k_{\parallel}^2/2m$$
$$=i\,|(2mE/\hbar^2)-k_{\parallel}^2|^{1/2};\quad E<\hbar^2k_{\parallel}^2/2m. \quad (123b)$$

The expressions for the bulk- and surface-plasmon contributions to the image potential, Σ_{bp} and Σ_{sp}, respectively, are immediate consequences of Eqs. (94) and (114). Considering the zero-temperature limit gives

$$\Sigma_{sp}(z,z';\vec{k}_{\parallel},E)=-\frac{i\pi e^2 m\hbar\omega_p}{\hbar^2 2^{1/2}}\int\frac{d^2q}{(2\pi)^2}\,\frac{e^{i\gamma_s|z-z'|}}{q\gamma_s}\times e^{-q(|z|+|z'|)}, \quad (124a)$$

$$\gamma_s^2=[2m(E-\hbar\omega_p/2^{1/2})/\hbar^2]-(\vec{k}_{\parallel}+\vec{q})^2, \quad (124b)$$

$$\Sigma_{bp}(z,z';k_{\parallel},E)=-\frac{i\pi e^2 m\hbar\omega_p}{\hbar^2}\int\frac{d^2q}{(2\pi)^2}\,\frac{e^{i\gamma_b|z-z'|}}{q\gamma_b}\times\theta(z)\,\theta(z')\,(e^{-q|z-z'|}-e^{-q(z+z')}), \quad (125a)$$

$$\gamma_b^2=[2m(E-\hbar\omega_p)/\hbar^2]-(\vec{k}_{\parallel}+\vec{q})^2. \quad (125b)$$

The square-root conventions for Eqs. (124b) and (125b) are given in Eqs. (123).

The semiclassical limit of these results is obtained by taking the $m\to\infty$ limit in Eqs. (123), i.e.,

$$G_{00}^{sc}(z,z';\vec{k}_{\parallel},E)=\delta(z-z')/E. \quad (126)$$

In this limit the relevant optical potentials are

$$\Sigma_{sp}(z,z';E=0)=-\delta(z-z')\,e^2(1-e^{-2p_{cs}|z|})/4|z|, \quad (127a)$$

$$\Sigma_{bp}(z,z';E=0)=-\theta(z)\,\delta(z-z')\,e^2\times\left(\frac{p_{cb}}{2}-\frac{1-e^{-2p_{cb}|z|}}{4z}\right). \quad (127b)$$

We use p_{cb} and p_{cs} to designate the maximum wave vector of the bulk and surface plasmons, respectively. Equations (127) illustrate three important results. First, as $|z|\gg p_{cs}^{-1}$, the optical potential due to the surface plasmons becomes the classical image potential both inside and outside the jellium-vacuum interface. Second, for $z\gg p_{cb}^{-1}$ inside the jellium, the image potential due to the surface plasmons is canceled exactly (screened) by bulk-plasmon contributions to the optical potential resulting from the orthogonality and completeness relations satisfied by the density fluctuations. Thus, the vanishing of the image potential inside the metal results from the same mathematical feature of the theory which led to the reduction of the forward-scattering–bulk-plasmon–emission cross section as described in Sec. IV B. Finally, Eqs. (127) show that the high-frequency step-density model leads to the correct semiclassical static ($E=0$) limit despite the fact that we expect $\lambda(q,\omega\to 0)$ rather than $\lambda(q\to 0,\omega)$ in Eq. (64) to describe the quantum theory of this limit.[41] Note that this limit does indeed lead to a local potential. However, it is purely real and is long range in contrast to Gersten's predictions.[46,47]

The origin of this result lies in our taking the semiclassical limit in the intermediate states of the electron's propagation as well as the initial and final states. Gersten's procedure[67] treats these two types of electronic states in an asymmetrical fashion. The intermediate electronic states must be treated quantum mechanically (either explicitly or implicitly via a dielectric

function), so that losses are possible, before a dissipative optical potential can be obtained.

In our quantum theory of the optical potential, there is an intimate connection between the range of its nonlocality and its dissipative character. For example, if $E < \hbar\omega_p/2^{1/2}$, the optical potential is real. The range of the nonlocality of the surface and bulk-plasmon contributions to it are determined by

$$K_s = i\gamma_s = (\{2m[(\hbar\omega_p/2^{1/2}) - E]/\hbar^2\} + (\vec{k}_{\parallel} + \vec{q}^2)^2)^{1/2}\,, \tag{128a}$$

$$K_b = -i\gamma_b = \{[2m(\hbar\omega_p - E)/\hbar^2] + (\vec{k}_{\parallel} + \vec{q})^2\}^{1/2}\,, \tag{128b}$$

respectively. Thus as $E \to 0$ the potential exhibits its shortest-range nonlocality. The two contributions become increasingly nonlocal as E increases to $\hbar\omega_s = \hbar\omega_p/2^{1/2}$ and $\hbar\omega_p$, respectively. Above the plasmon-emission threshold, the concept of the "range" of the nonlocality becomes ill defined due to the oscillatory character of the $e^{i\gamma|z-z'|}$ factors in Eqs. (124). Also note that at the plasmon-emission threshold energy, the diagonal term of the optical potential becomes complex. If $\vec{k}_{\parallel} = 0$, the diagonal term is purely imaginary when E increases to the extent that

$$k_i^2(E) = 2m(E - \hbar\omega_i)\hbar^2 > p_{ci}^2\,. \tag{129}$$

Although the imaginary part of the diagonal terms of a nonlocal potential [e.g., $\mathrm{Im}\Sigma_{sp}(z, z; \vec{k}_{\parallel}, E)$ in Eq. (124a)] are necessarily associated with a physical absorptive process, the fact that off-diagonal elements of such a potential are not real has no direct physical interpretation. Therefore the evalution of Σ_{sp} and Σ_{bp} in closed form via Eqs. (124) and (125) is not our immediate concern. Rather, we turn in the Sec. V E to an approximate solution of Eq. (111b) for the distorted wave basis, in order to examine the nature of the *effective* electron-solid force for electrons which are "far" from the jellium interface.

E. Electron Motion Far Outside the Surface; Quantum Derivation of Image Potential

In this section, we give an approximate solution for electron motion under the influence of the optical potential. In particular we demonstrate that far outside the surface the electron moves as if it were acted upon by the image potential.

If a charged particle is located at a sufficiently great distance z from a metal surface, no matter how great the particle's velocity v, the frequency which characterizes the electric field it induces at the surface is small, of $O(v/z)$. Consequently, the induced motion of the electrons in the metal is adiabatic. Thus we expect the electron effective potential to be the image potential. The derivation of the image potential given in Sec. V D applies only in the classical limit $m \to \infty$, $v = 0$. We derive a similar result, for a finite-mass moving electron, but solving the Schrödinger equation [equivalent to Eq. (111b)]

$$\left(E - \frac{\hbar^2 k_{\parallel}^2}{2m} + \frac{\hbar^2}{2m}\frac{d^2}{dz^2}\right)\phi_{\vec{k}}(z) = \int dz'\,\Sigma(z, z'; \vec{k}_{\parallel}, E)\,\phi_{\vec{k}}(z') \tag{130}$$

approximately in the asymptotic region $z \to \infty$. We then discuss the possibility of evaluating the leading correction to the image-force law. In this asymptotic region, the effective potential varies rather slowly compared to a fast electron's wave function. Thus we attempt a WKB-like solution of Eq. (130) by assuming $\phi_{\vec{k}}(z)$ to be of the form

$$\phi_{\vec{k}}(z) = e^{ik_\perp z} F_{\vec{k}}(z)\,, \tag{131a}$$

$$k_\perp = (2mE/\hbar^2 - k_{\parallel}^2)^{1/2}\,, \tag{131b}$$

where $F_{\vec{k}}$ is slowly varying in a sense to be defined. Substituting the *ansatz* (131a) in Eq. (130), we obtain

$$\frac{\hbar^2}{2m}\left(2ik_\perp\frac{dF_{\vec{k}}}{dz} + \frac{d^2F_{\vec{k}}}{dz^2}\right) = \int_{-\infty}^{\infty} dz'\,\Sigma(z, z'; \vec{k}_{\parallel}, E)\,e^{-ik_\perp(z-z')}F_{\vec{k}}(z')\,. \tag{132}$$

We now suppose that two criteria of slowness of $F_{\vec{k}}$'s variation are satisfied:

$$\left|\frac{d^2F_{\vec{k}}}{dz^2}\right| \ll 2k_\perp\left|\frac{dF_{\vec{k}}}{dz}\right|, \tag{133a}$$

$$\left[\left(\int dz'\,\Sigma(z, z'; \vec{k}_{\parallel}, E)\,e^{-ik_\perp(z-z')}F_{\vec{k}}(z')\right)/\int dz'\,\Sigma(z, z'; \vec{k}_{\parallel}, E)\,e^{-ik_\perp(z-z')}F_{\vec{k}}(z)\right] - 1\Big| \ll 1. \tag{133b}$$

The first [(133a)] is the criterion for the validity of the ordinary WKB approximation. The second [(133b)] permits us to replace $F_{\vec{k}}(z')$ by $F_{\vec{k}}(z)$ in Eq. (132); its validity, together with that of (133a), enables us to approximate the integral equation (132) by the differential equation

$$\frac{d}{dz}\left[\ln F_{\vec{k}}(z)\right] \approx \frac{m}{i\hbar^2 k_\perp}\int_{-\infty}^{\infty} dz'\,\Sigma(z, z'; \vec{k}_{\parallel}, E)\,e^{-ik_\perp(z-z')}\,. \tag{134}$$

We wish to integrate Eq. (134) in the asymptotic region $z \to \infty$ and to verify there the satisfaction of the inequalities (133) *a posteriori*. In the asymptotic region, cf. Eq. (125a), the bulk plasmons do not contribute to Σ, nor, of course, does the Hartree-Fock potential. Thus we replace Σ by Σ_{sp}, cf. Eq. (124a), and obtain

$$\frac{d}{dz}\left[\ln F_{\vec{k}}(z)\right] \approx -\frac{\pi e^2 m^2 \omega_p}{\hbar^3 2^{1/2} k_\perp} \int_{-\infty}^{\infty} dz'\, e^{-ik_\perp(z-z')} \times \int \frac{d^2q}{(2\pi)^2} \frac{\exp(i\gamma_s|z-z'|)}{q\gamma_s} e^{-q(|z|+|z'|)}. \quad (135)$$

Performing the z' integration in Eq. (135), we find

$$\frac{d}{dz}\left[\ln F_{\vec{k}}(z)\right] \approx -\frac{2\pi e^2 m^2 \omega_p}{\hbar^3 2^{1/2} k_\perp} \int \frac{d^2q}{(2\pi)^2} \frac{1}{q}\left(\frac{ie^{2qz}}{(ik_\perp+q)^2+\gamma_s^2} + q\frac{e^{(q-ik_\perp-i\gamma_s)z}}{\gamma_s[q^2+(k_\perp+\gamma_s^2)]}\right). \quad (136)$$

In order to take the limit of large (negative) z, we make the variable change

$$\vec{Q} = |z|\vec{q}\,, \quad (137)$$

which yields

$$\frac{d}{dz}\left[\ln F_{\vec{k}}(z)\right] = \frac{2\pi e^2 m^2}{\hbar^3 k_\perp}\frac{\omega_p}{2^{1/2}}\frac{1}{z}\int \frac{d^2Q}{(2\pi)^2}\frac{1}{Q}\left[-ie^{-2Q}\Big/\left(\frac{2m}{\hbar^2}\frac{\hbar\omega_p}{2^{1/2}} - \frac{2ik_\perp Q}{z} + \frac{2\vec{k}_\parallel Q}{z}\right) + \frac{Q}{z\gamma_s}\frac{e^{-Q-i(k_\perp+\gamma_s)z}}{Q^2/z^2+(k_\perp+\gamma_s)^2}\right]. \quad (138)$$

We have made use of Eqs. (124b) and (131b) in obtaining the denominator of the first term on the right-hand side of Eq. (138). In the limit $z \to -\infty$, this denominator approaches a constant $2m\omega_p/\hbar 2^{1/2}$ and the second term within the bracket vanishes.[70] Therefore, in the asymptotic region Eq. (138) reduces to

$$\frac{d}{dz}\left[\ln F_{\vec{k}}(z)\right] = -\frac{2\hbar\pi e^2 m^2}{\hbar^3 k_\perp}\frac{\omega_p}{2^{1/2}}\frac{1}{z}\frac{\hbar 2^{1/2}}{2m\omega_p} \times \int \frac{d^2Q}{(2\pi)^2}\frac{e^{-2Q}}{Q} = -\frac{ie^2 m}{4\hbar^2 k_\perp z}. \quad (139)$$

Integrating and substituting in Eq. (131a) we find the approximate wave function

$$\phi_{\vec{k}}(z) \approx \exp i\int^z dz'\left(k_\perp - \frac{e^2 m}{4\hbar^2 z'}\frac{1}{k_\perp}\right). \quad (140)$$

By comparison, the lowest-order WKB (continuum) wave function for an arbitary local potential $V(z)$ is given by

$$\phi(z) = \exp\left[i\int^z dz'\left(k_\perp^2 - \frac{2m}{\hbar^2}V(z')\right)^{1/2}\right], \quad (141)$$

where $k_\perp$ is the asymptotic electron wave vector. Assuming $V(z) \ll (\hbar^2 k_\perp^2/2m)$, we expand the square root in Eq. (141). This yields

$$\phi(z) = \exp\left[i\int^z dz'\left(k_\perp - \frac{m}{\hbar^2 k_\perp}V(z') + \cdots\right)\right]. \quad (142)$$

Comparing Eqs. (142) and (140), we see that in the asymptotic region $z \to -\infty$, the electron in the case (140) moves as if it were in a local potential

$$V(z) = \frac{e^2}{4z} = -\frac{e^2}{4|z|}. \quad (143)$$

Thus we have established the result stated at the outset, provided that the inequalities (133) can be shown to be valid.

We therefore proceed to determine the conditions under which these inequalities are satisfied. According to Eq. (139),

$$\left|\frac{d^2F_{\vec{k}}}{dz^2}\Big/\frac{dF_{\vec{k}}}{dz}\right| = \left|\left[\left(\frac{e^2m}{4\hbar^2k_\perp}\right)^2 - \frac{ie^2m}{4\hbar^2k_\perp z^2}\right]\Big/\frac{ie^2m}{4\hbar^2k_\perp z}\right| = \frac{1}{z}\left[1+\left(\frac{e^2m}{4\hbar^2k_\perp}\right)^2\right]^{1/2}. \quad (144)$$

Thus (133a) is satisfied if

$$k_\perp z \gg \frac{1}{2}\left[1+\left(\frac{e^2m}{4\hbar^2k_\perp}\right)^2\right]^{1/2}. \quad (145)$$

For a 40-eV electron, as an example, this requires

$$z \gg 0.3a_B \approx 0.15\ \text{Å}, \quad (146)$$

where a_B is the Bohr radius. Thus inequality (133a) is satisfied to distances which are well within the distance from the surface at which the image potential can no longer be a good representation of the effective potential.

In order to study the satisfaction of the second inequality (133b) we must evaluate the integral

$$M(z) \equiv \int dz'\, \Sigma_{sp}(z, z'; \vec{k}_\parallel, E)\, e^{-ik_\perp(z-z')} F_{\vec{k}}(z'), \quad (147)$$

in which we use, cf. Eq. (139),

$$F_k(z') = (z')^{-ie^2m/4\hbar^2k_\perp}. \quad (148)$$

The integral may be carried out exactly to give (in terms of incomplete Γ functions)[71]

$$M(z) = \frac{-i\pi}{a_B}\frac{\hbar\omega_p}{2^{1/2}}\int\frac{d^2q}{(2\pi)^2}\frac{1}{q\gamma_s}\left[\frac{2i\gamma_s}{(q+ik_\perp)^2+\gamma_s^2}\right. e^{2qz} z^{-ip}$$

$$+e^{-i(\gamma_s+k_\perp)z+qz}\Gamma(1-ip)\left(\frac{1}{[-i(\gamma_s+k_\perp)+q]^{1-ip}}-\frac{1}{[-i(\gamma_s+k_\perp)-q]^{1-ip}}\right)$$

$$+ipe^{(-ik_\perp+q)z}\left(\frac{e^{i\gamma_s z}\Gamma(-ip, i(\gamma_s-k_\perp)z-qz)}{[i(\gamma_s-k_\perp)-q]^{1-ip}}-\frac{e^{-i\gamma_s z}\Gamma(-ip,-i(\gamma_s+k_\perp)z-qz)}{[-i(\gamma_s+k_\perp)-q]^{1-ip}}\right)\Bigg], \quad (149)$$

in which we have defined

$$p\equiv\frac{e^2m}{4\hbar^2k_\perp}=\frac{1}{4a_Bk_\perp}, \quad (150)$$

and in which the incomplete and complete Γ functions, respectively, are given by

$$\Gamma(\alpha, x)\equiv\int_x^\infty dt\, e^{-t}t^{\alpha-1},$$
$$\Gamma(\alpha)\equiv\Gamma(\alpha, 0). \quad (151)$$

We may obtain from Eq. (149) a simpler expression for $M(z)$, valid in the asymptotic region $z\to-\infty$, by using the formula

$$\Gamma(\alpha, x)\underset{x\to\infty}{\longrightarrow}x^{\alpha-1}e^{-x}[1+O(1x)]. \quad (152)$$

That is,

$$M(z)\underset{z\to-\infty}{\longrightarrow}\frac{-i\pi}{a_B}\frac{\hbar\omega_p}{2^{1/2}}\int\frac{d^2q}{(2\pi)^2}\frac{1}{q\gamma_s}\Bigg[2i\gamma_s e^{2qz}z^{-ip}\Big/\left(\frac{2m}{\hbar^2}\frac{\hbar\omega_p}{2^{1/2}}-2ik_\perp q+2\vec{k}_\parallel\cdot\vec{q}\right)-\frac{2q\Gamma(2-ip)}{[-i(\gamma_s+k_\perp)]^{2-ip}}\times e^{-i(\gamma_s+k_\perp)z+qz}-\frac{2ip\gamma_sk_\perp\hbar^2}{m^2\omega_p^2}z^{-1-ip}\Bigg]. \quad (153)$$

In order to show that the inequality (133b) is satisfied we must demonstrate that $M(z\to\infty)$ is nearly equal to z^{-ip} times the integral $\int dz'\,\Sigma_{sp}(z, z';\vec{k}_\parallel, E)e^{-ik_\perp(z-z')}$, which we have already calculated [cf. Eqs. (134) and (136)]. In the asymptotic region, z^{-ip} times this integral equals

$$-\frac{i\pi}{a_B}\frac{\hbar\omega_p}{2^{1/2}}\int\frac{d^2q}{(2\pi)^2}\frac{1}{q\gamma_s}\left[2i\gamma_s e^{2qz}z^{-ip}\Big/\left(\frac{2m}{\hbar^2}\frac{\hbar\omega_p}{2^{1/2}}-2ik_\perp q+2\vec{k}\cdot\vec{q}\right)+\frac{2qz^{-ip}e^{qz-i(k_\perp+\gamma_s)z}}{(\gamma_s+k_\perp)^2}\right]. \quad (154)$$

Note that for sufficiently large $|z|$, only the first terms within the respective brackets of (153) and (154) contribute. But these terms are identical. Therefore, at sufficiently large values of $|z|$, the inequality (133b) is satisfied. This completes the quantum-mechanical demonstration that sufficiently far outside a solid surface an electron moves as though it were under the influence of the image potential.

Finally we note that the difference between (153) and (154) is comparable in magnitude to the second term in the bracket of (154). But this latter term represents a typical correction to the image potential. Thus it appears that the error inherent in our WKB method is comparable to the magnitude of the corrections to the image potential. This implies that we cannot utilize a local approximation to Eq. (130) if we wish to evaluate accurately corrections to the image-force law.

VI. SYNOPSIS

In this paper we have laid the foundation for a microscopic theory of low-energy electron diffraction in which the consequences of both surface and bulk inelastic loss processes are incorporated in a natural way. The formalism which we use was reviewed in Sec. II. In Sec. III, we classified models of the loss processes, related the assumptions and construction of the models to each other, and compared their predictions. In Sec. IV we demonstrated that one of these models, the high-frequency step-density model, led naturally both to the semiphenomenological inelastic-collision model of ILEED[8] and to the prediction of the observed[53] reduction in the inelastic forward-scattering cross sections of keV electrons. In Sec. V, we developed a distorted-wave theory of ELEED, classified models of the optical potential used in this theory, displayed the approximations needed to reduce the full theory to models whose use is common in the literature, and provided a more accurate evaluation of the electron-electron-interaction induced optical potential as well as the demonstration that our evaluation of this potential reduced to the image force in all appropriate limits. The next logical step in the development of the theory is the solution to the Schrödinger equation obtained using our more accurate optical potential and a simple model of the short-range electron-ion-core interactions.

APPENDIX

One of our principal concerns in this paper has been to derive vertex functions which permit the

calculation of electron excitation of bulk and surface plasmons. In Sec. II, we derived such functions within the context of a hydrodynamic theory of the electron gas, in which dispersive effects were neglected. In this Appendix we discuss the inclusion of dispersion.

We find that in order to include dispersive effects, our description of unforced modes of electron-gas oscillation only needs minor modification. However, when we turn on an external field, in the dispersive theory, we find that the field appears not only as a source term in the hydrodynamic wave equation, but also in the boundary conditions at the electron-gas's surface. As a result, when there is dispersion, it is not straightforward to describe the gas's linear response in terms of its free-oscillation modes.

The basic equations of hydrodynamics are those of mass and momentum conservation, respectively,

$$\frac{\partial u}{\partial t} = -\vec{\nabla}\cdot(n_0\vec{w}), \tag{A1}$$

$$mn_0\frac{\partial\vec{w}}{\partial t} = -n_0\vec{\nabla}\phi - \vec{\nabla}p. \tag{A2}$$

As in the main text, u and $\vec{w}$ are the electron-density and velocity fluctuations, n_0 is the ground-state electron-density profile taken to be

$$n_0(z) = n_\infty\theta(z), \tag{A3}$$

and ϕ is the induced electrostatic potential, which solves Poisson's equation,

$$\nabla^2\phi = -4\pi e^2 u. \tag{A4}$$

The step-density model is completed by the assumption that the pressure fluctuation is given by the local constitutive relation

$$p = m\beta^2 u, \tag{A5}$$

where the constant β^2 is given by

$$\beta^2 = \tfrac{3}{5}v_F^2, \tag{A6}$$

a value which is chosen in order that the bulk-plasmon dispersion relation in the present case will agree with that of the RPA for the infinite-electron gas. Note that the fluctuating quantities $u, \vec{w}$, and p are only defined in the occupied half-space $z>0$, whereas ϕ is defined for all values of z.

Combining Eqs. (A1) and (A2), we find that

$$m\frac{\partial^2 u}{\partial t^2} = \vec{\nabla}\cdot(n_0\vec{\nabla}\phi) + \nabla^2 p. \tag{A7}$$

Expanding the expression $\vec{\nabla}\cdot(n_0\vec{\nabla}\phi)$ in Eq. (A7), and substituting Eqs. (A3)–(A5), we obtain

$$\frac{\partial^2 u}{\partial t^2} = -\omega_p^2\theta(z)u + \beta^2\nabla^2 u + \frac{n_\infty}{m}\delta(z)\frac{d\phi}{dz}. \tag{A8}$$

The first question that must be answered at this point is whether or not Eq. (A8) can be construed to be valid for $z\geq 0$ or only for $z>0$.

In more familiar problems that involve discontinuous or singular potentials, e.g., the quantum-mechanical square well, the matching conditions at the discontinuity are automatically generated by the differential equation under consideration (Schrödinger's equation in the square-well case). Boundary conditions need be specified only at infinity. In the present case, however, matching conditions cannot consistently be generated by the differential equation (A8) unless $u(z)\to 0$, as $z\to 0$ from the right. Otherwise, if $u(z)$ must behave like a constant times $\theta(z)$ as $z\to 0^+$, then (d^2u/dz^2) must behave like $\delta'(z)$ at $z=0$, and Eq. (A8) has no solution. In the case of the surface plasmon, we will see presently that $u(z)$ is *required* not to vanish as $z\to 0^+$. Thus Eq. (A8) can be construed to hold only in the interior of the solid, i.e., for $z>0$. Thus Eq. (A8) is rewritten

$$\frac{\partial^2 u}{\partial t^2} = -\omega_p^2 u + \beta^2\nabla^2 u \qquad z>0 \tag{A9}$$

and the hydrodynamic theory must be completed by the introduction of a boundary condition at $z=0^+$.

The boundary condition which is generally assumed is that the electron velocity in the z direction must vanish at $z=0^+$. The rationalization for this assumption is that electrons must not leave or enter the solid. It is equivalent, however, to the requirement that $u(z)$ contain no term proportional to $\delta(z)$, as may be seen by integrating the equation of continuity (A1) in a pillbox about the surface $z=0$. In any case, whether one chooses to ascribe the boundary condition

$$w_z(0^+) = 0 \tag{A10}$$

to the confinement of the electron fluid to the solid or to the absence of any δ-function-like surface-charge fluctuation, the real motivation for using Eq. (A10) to fix solutions of Eq. (A9) is that this procedure yields the correct infinite-wavelength surface-plasmon frequency.

We first proceed to solve Eqs. (A9) and (A10) for the surface and bulk modes of plasma oscillation. Note that the boundary condition (A10) together with Eq. (A2) implies that

$$-n_\infty\left.\frac{d\phi}{dz}\right|_{0^+} = \left.\frac{dp}{dz}\right|_{0^+}. \tag{A11}$$

Using Eq. (A5) and the solution of Poisson's equation [cf. Eq. (28)],

$$\phi(qz\omega) = \frac{2\pi e^2}{q}\int_0^\infty dz' e^{-q|z-z'|}u(qz'\omega), \tag{A12}$$

the condition (A11) may be rewritten

$$\left.\frac{du(qz\omega)}{dz}\right|_{z=0^+} = -\frac{\omega_p^2}{2\beta^2}\int_0^\infty dz' e^{-qz'} u(qz'\omega), \quad \text{(A13)}$$

a form which involves only the unknown function u. We Fourier transform Eq. (A9) in $\vec{x}$ and t, obtaining

$$\left(\omega^2 - \omega_p^2 - \beta^2 q^2 + \beta^2 \frac{d^2}{dz^2}\right) u(qz\omega) = 0. \quad \text{(A14)}$$

Equations (A13) and (A14) are the well-known linearized hydrodynamic equations for the semi-infinite electron gas.

A surface mode corresponds to a solution of Eqs. (A13) and (A14) which vanishes at $z=\infty$. We see immediately that there is only one possible *ansatz* for the charge fluctuation,

$$u(qz\omega) = u_s e^{-\gamma z}, \quad \text{(A15)}$$

where u_s is a normalization constant. [This form of $u(qz\omega)$ substantiates our earlier remark that for a surface mode, $u(z)\to 0$ as $z\to 0^+$ is not possible.] In order that Eq. (A15) be consistent with Eq. (A14), it is necessary that

$$\omega^2 = \omega_p^2 + \beta^2(q^2 - \gamma^2). \quad \text{(A16)}$$

In order that it be consistent with the boundary condition (A13), however, it must be true that

$$\gamma = \frac{\omega_p^2}{2\beta^2}\frac{1}{q+\gamma}. \quad \text{(A17)}$$

Solving for γ, Eq. (A17) yields

$$\gamma = \left(\frac{\omega_p^2}{2\beta^2} + \frac{q^2}{4}\right)^{1/2} - \frac{q}{2}. \quad \text{(A18)}$$

Substituting from Eq. (A18) into Eq. (A16), we find the surface-mode dispersion relation

$$\omega^2 = \tfrac{1}{2}\omega_p^2 + \beta q\,(\tfrac{1}{2}\omega_p^2 + \tfrac{1}{4}\beta^2 q^2)^{1/2} + \tfrac{1}{2}\beta^2 q^2, \quad \text{(A19)}$$

which is Ritchie's hydrodynamic result. The fact that at $q=0$ we find $\omega^2 = \frac{1}{2}\omega_p^2$ leads us to identify the surface mode as the well-known surface plasmon; this result, of course, was obtained by the imposition of the boundary condition (A13).

The bulk-mode solutions to the hydrodynamic equations also can be found easily. These modes are expected to vary sinusoidally as $z\to\infty$. The most general bulk mode that can satisfy Eq. (A14) is thus given by

$$u_k(qz\omega) = u_b \sin(Kz + \alpha), \quad \text{(A20)}$$

where u_b is an arbitrary normalization constant and α, the phase, is to be determined by the satisfaction of Eq. (A13). In order that (A20) solve Eq. (A14), of course, it is necessary that

$$\omega^2 = \omega_p^2 + \beta^2(q^2 + K^2), \quad \text{(A21)}$$

which is the ordinary bulk-plasmon dispersion relation. Substituting Eq. (A20) into Eq. (A13), we see that α must satisfy

$$K\cos\alpha = \frac{-\omega_p^2}{2\beta^2}\,\frac{q\sin\alpha + K\cos\alpha}{q^2+K^2}. \quad \text{(A22)}$$

The resulting value of α substituted in Eq. (A20) yields the bulk-mode density fluctuation

$$u_k(qz\omega) = \frac{u_0\cos\alpha}{q} \times\left[q\sin Kz - K\left(1 + \frac{2\beta^2(q^2+K^2)}{\omega_p^2}\right)\cos Kz\right]. \quad \text{(A23)}$$

Note that in the dispersionless limit ($\beta^2\to 0$), choosing the normalization $u_0\cos\alpha = q$, this result reduces to our earlier one, Eq. (54b) of Sec. III B. The fact that it does not reduce to Gersten's $u_K^{(B)}$ [cf. Eq. (69) of Sec. III B] is not an accident; that is guaranteed by the boundary condition (A10), which is equivalent to the requirement that u not contain a term proportional to $\delta(z)$.

At this point, we have determined *all* of the solutions of Eqs. (A13) and (A14). In order to show that they constitute a complete orthogonal set of eigenmodes, we must define a scalar product (f_1, f_2) in the space of functions f satisfying the boundary condition (A13), we must then demonstrate that the operator d^2/dz^2 is Hermitian in this space.

Evidently, if we choose the "wrong" definition of the scalar product, the proof of Hermiticity will fail. If, for example, in analogy to our previous results, we define

$$(f_1, f_2)_0 \equiv \frac{2\pi e^2}{q}\int dz\,dz' f_1(z) e^{-q|z-z'|} f_2(z'), \quad \text{(A24)}$$

where the subscript 0 stands for $\beta^2 = 0$, it is easy to see that

$$\left(\frac{d^2 f_1}{dz^2}, f_2\right)_0 \neq \left(f_1, \frac{d^2 f_2}{dz^2}\right)_0. \quad \text{(A25)}$$

The *ansatz* with respect to which d^2/dz^2 is a Hermitian operator is

$$(f_1, f_2)_{\beta^2} \equiv \frac{2\pi e^2}{q}\int_0^\infty dz \int_0^\infty dz' f_1(z)(e^{-q|z-z'|} + e^{-q(z+z')}) f_2(z'). \quad \text{(A26)}$$

Starting with Eq. (A26), it is easy to verify that

$$\left(\frac{d^2 f_1}{dz^2}, f_2\right)_{\beta^2} - \left(f_1, \frac{d^2 f_2}{dz^2}\right)_{\beta^2} = -\frac{4\pi e^2}{q}\left(\left.\frac{df_1}{dz}\right|_0 \int_0^\infty dz' e^{-qz'} f_2(z') - \left.\frac{df_2}{dz'}\right|_0 \times \int_0^\infty dz\, e^{-qz} f_1(z)\right). \quad \text{(A27)}$$

However, as a consequence of the assumption that

f_1 and f_2 satisfy the boundary condition (A13), the right-hand side of Eq. (A27) vanishes, which implies that d^2/dz^2 is Hermitian. It also implies that the solutions to the hydrodynamic equations with $\beta^2 \neq 0$ are orthogonal with respect to the condition

$$(u_l, u_{l'})_{\beta 2} = 0, \quad l \neq l' . \tag{A28}$$

This fact raises the question of how the $\beta^2 = 0$ limit is approached, for β^2 does not appear explicitly in the definition (A26), and we know that at $\beta^2 = 0$ the solutions to hydrodynamic equations are orthogonal with respect to the scalar product of Eq. (A24). This paradox is resolved by the observation that the $\beta^2 = 0$ hydrodynamic solutions are in fact *also* orthogonal with respect to the scalar product of Eq. (A26). Thus a $\beta^2 = 0$ hydrodynamic theory could have been based on the orthogonality relation of Eq. (A26) as well as on that of Eq. (A24).

This completes our discussion of the free oscillations of the semi-infinite electron gas within the hydrodynamic model including dispersion. The logical next step is to consider the excitation of these oscillations by an external potential, and, in particular, to obtain the density-density response function which is the $\beta^2 \neq 0$ extension of that of Eq. (64).

Turning on an external potential $V_{\mathrm{EXT}}(\vec{x}, t)$ modifies the Euler equation (A2) but does not affect the other hydrodynamic equations (A1), (A4), and (A5). Equation (A2) is replaced by

$$mn_0 \frac{\partial \vec{w}}{\partial t} = -n_0 \vec{\nabla}\phi - n_0 \vec{\nabla} V_{\mathrm{EXT}} - \vec{\nabla} p , \tag{A29}$$

and, as a result, the wave equation (A14) is replaced by

$$\left(\omega^2 - \omega_p^2 - \beta^2 q^2 + \beta^2 \frac{d^2}{dz^2}\right) u(qz\omega) = \frac{n_\infty}{m}\left(\frac{d^2}{dz^2} - q^2\right) V_{\mathrm{EXT}}(qz\omega) . \tag{A30}$$

However, the boundary condition (A14) is *also* modified by turning on V_{EXT}, since according to Eq. (A29) the condition Eq. (A10) now implies that

$$-n_\infty \left.\frac{d\phi}{dz}\right|_{0^+} = \left.\frac{dp}{dz}\right|_{0^+} + n_\infty \left.\frac{dV_{\mathrm{EXT}}}{dz}\right|_{0^+} . \tag{A31}$$

As a result of this change in the boundary condition, the solutions of Eqs. (A30) and (A31) cannot simply be expanded as a linear combination of the solutions of Eqs. (A13) and (A14). The evaluation of the linear-response function in the dispersive hydrodynamic theory thus requires a modification of the procedures that are described in the main text, and for that reason it is not discussed here.

---

*Work supported in part by the Advanced Research Projects Agency under Contract No. HC 15-67-C-0221, and by the Army Research Office (Durham) under Contract No. DA-HC04-69 C007.

†Present address: James Franck Institute, University of Chicago, Chicago, Ill. 60637.

[1]P. J. Estrup and E. G. McRae, Surface Sci. 25, 1 (1971).

[2]C. B. Duke and C. W. Tucker, Jr., Phys. Rev. B 3, 3561 (1971).

[3]S. Y. Tong and T. N. Rhodin, Phys. Rev. Letters 26, 711 (1971).

[4]D. W. Jepsen, P. M. Marcus, and F. Jona, Phys. Rev. Letters 26, 1365 (1971).

[5]J. A. Strozier, Jr. and R. O. Jones, Phys. Rev. B 3, 3228 (1971).

[6]G. Capart, Surface Sci. 26, 429 (1971).

[7]G. E. Laramore, C. B. Duke, A. Bagchi, and A. B. Kunz, Phys. Rev. B 4, 2058 (1971).

[8]C. B. Duke and G. E. Laramore, Phys. Rev. B 3, 3183 (1971).

[9]G. E. Laramore and C. B. Duke, Phys. Rev. B 3, 3198 (1971).

[10]C. W. Tucker, Jr. and C. B. Duke, Surface Sci. 23, 411 (1970).

[11]C. B. Duke and C. W. Tucker, Jr., J. Vac. Sci. Technol. 8, 5 (1971).

[12]M. G. Lagally, T. C. Ngoc, and M. B. Webb, Phys. Rev. Letters 26, 1557 (1971).

[13]C. B. Duke and A. Bagchi, J. Vac. Sci. Technol. (to be published).

[14]A. Bagchi, C. B. Duke, P. J. Feibelman, and J. O. Porteus, Phys. Rev. Letters 27, 998 (1971).

[15]C. B. Duke and C. W. Tucker, Jr., Surface Sci. 15, 231 (1969).

[16]G. E. Laramore and C. B. Duke, Phys. Rev. B 4, 2058 (1971).

[17]G. E. Laramore, J. Vac. Sci. Technol. (to be published).

[18]P. A. Fedders, Phys. Rev. 153, 438 (1967).

[19]P. J. Feibelman, Phys. Rev. 176, 551 (1968).

[20]A. V. Sidyakin, Zh. Eksperim. i Teor. Fiz. 58, 573 (1970) [Sov. Phys. JETP 31, 308 (1970)].

[21]D. M. Newns, Phys. Rev. B 1, 3304 (1970); also J. Rudnick, Ph.D. thesis (University of California, San Diego, 1969) (unpublished).

[22]D. E. Beck and V. Celli, Phys. Rev. B 2, 2955 (1970).

[23]J. Harris and A. Griffin, Can. J. Phys. 48, 2592 (1970).

[24]V. Peuckert, Z. Physik 241, A1 (1971).

[25]See, e.g., H. Raether, Ergeb. Exakt. Naturw. 38, 84 (1965); Colloque J. Phys. 31, 59 (1970).

[26]C. Kunz, Phys. Status Solidi 1, 441 (1961).

[27]R. H. Ritchie, Phys. Rev. 106, 874 (1957).

[28]L. Van Hove, Phys. Rev. 95, 249 (1954).

[29]E. A. Stern and R. A. Ferrell, Phys. Rev. 120, 130 (1960).

[30]The method used has been introduced in earlier work. See, e.g., P. J. Feibelman, Ann. Phys. (N.Y.) 48, 389 (1968); also Ref. 19.

[31a]D. E. Beck, Phys. Rev. B 4, 1555 (1971).

[31b]Ch. Heger and D. Wagner, Z. Physik 244, 499 (1971).

[32]The factor of 2 in Eq. (7) takes account of spin summation. This remark also applies to Eq. (3).

[33]In fact, a self-consistent solution for $n_0(z)$ probably does not exist because we have neglected exchange and

correlation energies [see, e.g., C. B. Duke, J. Vac. Sci. Technol. 6, 152 (1969)]. Nevertheless, we proceed as if there were a solution.

[34]D. E. Beck, V. Celli, G. LoVecchio, and A. Magnaterra, Nuovo Cimento 68B, 230 (1970).

[35]P. J. Feibelman, Phys. Rev. B 3, 220 (1971).

[36]P. J. Feibelman, Phys. Rev. B 3, 2974 (1971).

[37]By symmetry of the n and n' sums and of the integral on $\vec{k}$.

[38]In coordinate space, $\langle z|f_q|z'\rangle = (4\pi e^2)^{1/2}K_0(q[z-z'])$, where K_0 is the zero-order Bessel function of imaginary argument.

[39]D. E. Beck (private communication).

[40]We have left out the force due to internal pressure, p, which adds a term $-\nabla p$ to the right-hand side of Eq. (30). This term is responsible for plasmon dispersion. It is neglected in the present case, for comparison with $O(1/\omega^2)$ RPA high-frequency approximation, which contains no dispersion corrections.

[41]P. J. Feibelman, Surface Sci. 27, 438 (1971).

[42]See the Appendix; also, J. Harris, Phys. Rev. B 4, 1022 (1971).

[43]A. J. Bennett, Phys. Rev. B 1, 203 (1970).

[44]B. Roulet and P. Nozieres, J. Phys. Radium 29, 167 (1968).

[45]The superscripts (S) and (B) denote surface and bulk modes, respectively.

[46]J. I. Gersten, Phys. Rev. 188, 774 (1969).

[47]C. B. Duke, G. E. Laramore, and V. Metze, Solid State Commun. 8, 1189 (1969).

[48]C. B. Duke, A. J. Howsmon, and G. E. Laramore, J. Vac. Sci. Technol. 8, 10 (1971).

[49]See Ref. 13.

[50]See Ref. 14.

[51]A. A. Abrikosov, L. P. Gorkov, and I. E. Dzyaloshinski, *Methods of Quantum Field Theory in Statistical Physics*, translated by R. A. Silverman (Prentice Hall, Englewood Cliffs, N. J., 1963).

[52]See, e.g., C. B. Duke, M. J. Rice, and F. Steinrisser, Phys. Rev. 181, 733 (1969).

[53]C. Kunz, Z. Physik 167, 53 (1962).

[54]P. Schmüser, Z. Physik 180, 105 (1964).

[55]H. Raether, Ergeb. Exakt. Naturw. 38, 84 (1965).

[56]J. Geiger and K. Wittmaack, Z. Physik. 195, 44 (1966).

[57]R. A. Ferrell, Phys. Rev. 101, 554 (1956).

[58]J. S. Bell and E. J. Squires, Phys. Rev. Letters 3, 96 (1959).

[59]N. F. Mott and H. S. W. Massey, *The Theory of Atomic Collisions*, 3rd ed. (Clarendon, Oxford, 1965), Chap. 13.

[60]L. Hedin and S. Lundquist, Solid State Phys. 23, 2 (1969).

[61]C. B. Duke, J. Vac. Sci. Technol. 6, 152 (1969).

[62]J. Bardeen, Phys. Rev. 58, 727 (1940).

[63]R. G. Sachs and D. L. Dexter, J. Appl. Phys. 21, 1304 (1950).

[64]See Ref. 20.

[65]N. Takimoto, Phys. Rev. 146, 366 (1966).

[66]A. A. Lucas and M. Sunjić, Phys. Rev. Letters 26, 229 (1971).

[67]J. I. Gersten, Phys. Rev. B 2, 3457 (1970).

[68]A. A. Lucas, Phys. Rev. Letters 26, 813 (1971).

[69]J. L. Beeby, J. Phys. C 1, 82 (1968).

[70]As $|z| > \infty$ the second term vanishes as $1/|z|$, except at the surface-plasmon threshold, given by $E - \hbar\omega_p/\sqrt{2} = \hbar^2k^2/2m$. In this case it falls off only as $z^{-1/2}$.

[71]I. S. Gradshteyn and I. M. Ryzhik, *Tables of Integrals Series and Products* (Academic, New York, 1965), p. 940.

[72]R. H. Ritchie, Progr. Theoret. Phys. (Kyoto) 29, 607 (1960).

PHYSICAL REVIEW B VOLUME 5, NUMBER 7 1 APRIL 1972

Mössbauer Effect of ^{57}Fe in Cubic $Cd_{0.98}Fe_{0.02}Cr_2S_4$

A. M. van Diepen and R. P. van Stapele
Philips Research Laboratories, Eindhoven, Netherlands
(Received 8 November 1971)

Mössbauer spectra of $Cd_{0.98}Fe_{0.02}Cr_2S_4$, taken between 5 and 300 K, reveal that there is a magnetically induced, temperature-dependent quadrupole interaction below the Curie temperature (96 K). The observed temperature dependence of eQV_{zz} and H_{hf} can be understood in terms of the combined action of a crystal field, an exchange field, and a spin-orbit interaction. The following constants are derived: $\delta = 6(\lambda^2/\Delta_c + \rho) = 12$ cm^{-1}, $eQV_{zz}(0) = 5.75$ mm/sec, $E_{ex}(0) = 90$ K, $\lambda = 62$ cm^{-1}, $Q = 0.24 \times 10^{-24}$ cm^2, and $2\kappa = 0.83$. Within experimental error the principal axis of the electric field gradient is parallel to the hyperfine field.

I. INTRODUCTION

Mössbauer spectra of ^{57}Fe in $FeCr_2S_4$ have been reported by several authors,[1-3] but up till now the results are not completely understood. The compound has the spinel structure, Fe being at the tetrahedral A sites. Magnetization data on a single crystal reveal that below the Curie point the preferred direction of the magnetization is the [100] direction.[3] It can be shown that a combination of a crystal field, an exchange field, and a spin-orbit interaction then gives rise to an induced electric field gradient (EFG) at the nucleus, axially symmetric around the direction of the hyperfine field